

Fig. 1. Development of FV-induced disease in CB6F₁ mice and its prevention by immunization with the single-epitope peptide i. (a) CB6F₁ mice were inoculated intravenously with 15 ($n = 11$), 50 ($n = 10$) or 150 SFFU ($n = 10$) of FV and the survival of infected animals was examined. Similar curves were obtained in three repeated experiments. For a comparison, (B10.A × A.BY)_{F1} ($n = 40$) mice were also infected with 15 SFFU of FV and followed for their survival until PID 90. (b) The effect of different doses of peptide i on protective immunity against FV. CB6F₁ mice were immunized once with 1, 3 or 10 μg per mouse of peptide i in CFA, or given a CFA emulsion of purified F-MuLV particles at 40 μg per mouse. The F-MuLV particles used had been inactivated by UV irradiation as described (19). Control mice were given CFA without any peptide (CFA alone). Mice were challenged with 150 SFFU FV 4 weeks after immunization, and their spleen weight was measured as soon as they died (CFA alone group) or were killed at PID 45. Significant differences in spleen weights were only observed between the CFA alone group and five other groups ($P < 0.006$). (c) Changes in the percentages of TER-119⁺ erythroid cells among nucleated spleen cells of FV-infected CB6F₁ mice. Mice were immunized once with 10 μg (5 nmol) of peptide i in CFA or given CFA alone and inoculated with FV 4 weeks later. Each data point shows mean \pm SEM calculated by using four to five individual mice per group. (d) Changes in serum titers of virus-neutralizing IgM and IgG antibodies after FV infection. CB6F₁ mice were either immunized once with 10 μg per mouse peptide i in CFA or given CFA alone, and challenged with 150 SFFU FV 4 weeks later. Each data point shows mean \pm SEM calculated by using seven to eight individual mice per group. Serum titers of F-MuLV-neutralizing IgM and IgG were compared by paired *t*-test: *IgM titers are significantly higher than IgG titers at $P < 0.05$; ** $P < 0.0001$. †, IgG titers are significantly higher than IgM titers at $P < 0.05$; ‡, $P < 0.01$.

CB6F₁ mice, CD4⁺ and CD8⁺ T cells were purified from CB6F₁ mice at 3 weeks after a single immunization with peptide i, and re-stimulated *in vitro* in the presence of syngeneic, γ -irradiated spleen cells as antigen-presenting cells (APCs). As shown in Fig. 2(a), CD4⁺ T cells purified from the immunized CB6F₁ mice proliferated vigorously when stimulated with 1 μM of peptide i, while the proliferative responses of CD4⁺ T cells purified from the control mice given CFA alone were below the background level even when stimulated with 20 μM of the same peptide. As controls, CD8⁺ T cells purified either from the peptide-immunized or unimmunized control mice showed no significant proliferative responses even when stimulated with 20 μM peptide i.

To determine the minimal amount of the peptide that is required for the effective induction of protective immunity

against FV infection, three different amounts of peptide i were given as a single intradermal immunization to CB6F₁ mice, and immunized mice were challenged with 150 SFFU FV. Since most of the unimmunized CB6F₁ mice died by PID 45 (Fig. 1a), infected mice were either dissected soon after their death or killed at PID 45, and their spleen weight was measured. As shown in Fig. 1(b), a single immunization with 3 μg (1.7 nmol) per mouse of peptide i was as effective as 10 μg per mouse of the same peptide, and only one mouse among the ten that were given 1 μg peptide i developed splenomegaly after FV infection. Thus, in the following experiments, 3–10 μg per mouse of peptide i was used as a sufficiently large protective dose.

FV-induced early splenomegaly is caused by the rapid growth and differentiation of SFFV-infected erythroid progenitor

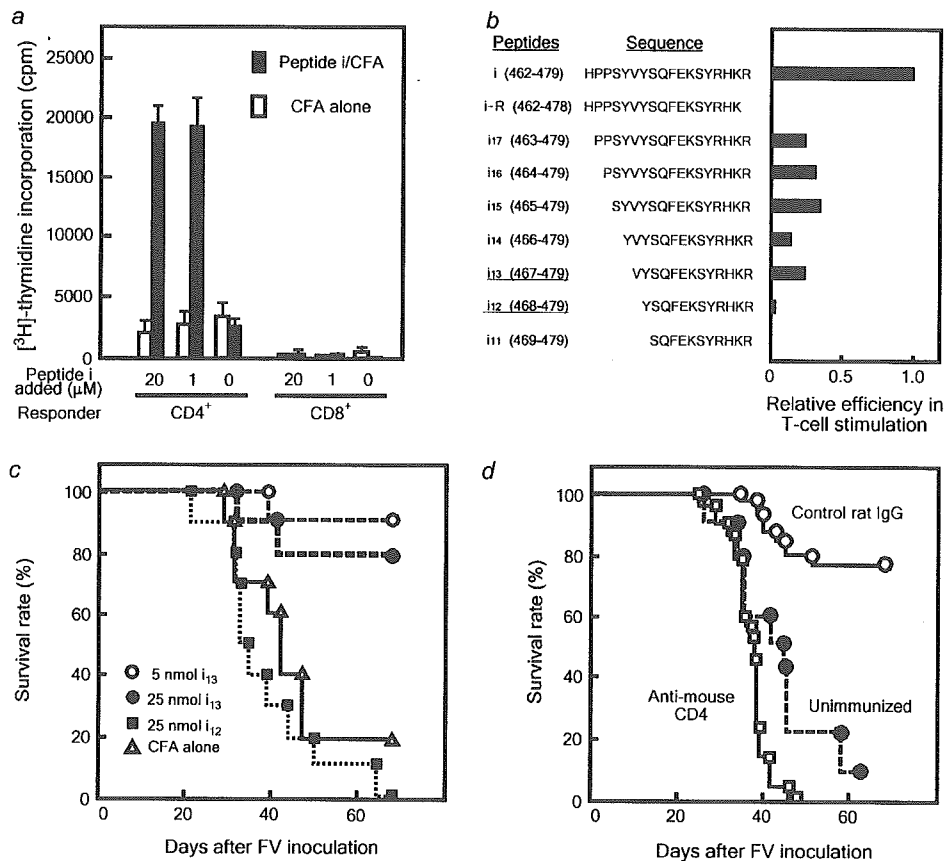


Fig. 2. Priming of CD4⁺ T cells by peptide immunization and efficacies in CD4⁺ T cell stimulation *in vitro* and immune protection *in vivo* of peptide i and its truncated derivatives. (a) Both CD4⁺ and CD8⁺ T cells were purified from the spleen of CB6F₁ mice at 3 weeks after a single immunization with 10 μg per mouse peptide i emulsified in CFA. Proliferative responses were measured 2 days after stimulation with the indicated concentration of peptide i along with syngeneic, γ-irradiated spleen cells as APCs. CD4⁺ and CD8⁺ T cells purified from CB6F₁ mice given CFA without a peptide (CFA alone) were used as controls. Data shown are averages + SEM of triplicate cultures, and the experiments were performed three times with essentially the same results. (b) Sequences of peptide i and its truncated derivatives, and their relative efficiency to stimulate FV-specific T cell clones. Representative data obtained with clone F5-5 are shown, while the data obtained with clone FP7-11 were consistent with those presented here. ED₅₀ of the full-length i was 0.2 μM. (c) Protection of CB6F₁ mice against FV infection with the truncated peptide. CB6F₁ mice (n = 10 per group) were immunized once with 5 nmol per mouse of peptide i₁₃, 25 nmol per mouse of i₁₃ or 25 nmol per mouse of i₁₂. Control mice were given CFA emulsion containing no peptide. Four weeks later, they were inoculated with 150 SFFU FV and followed for their survival. (d) CB6F₁ mice (n = 22 per group) were immunized once with 3 μg per mouse of peptide i and repeatedly injected with the anti-CD4 mAb (□) or control rat IgG (○). Four weeks after immunization, these mice and a group of unimmunized control mice (●) were inoculated with 150 SFFU FV and followed for their survival.

cells, and the resultant erythroblasts and maturing red cells are marked by mAb TER-119 (27). Thus, bursting of the TER-119⁺ erythroid cells was observed in the unimmunized control mice starting from PID 7, following the slow initial increase of the same cell population (Fig. 1c). On the other hand, the number of TER-119⁺ erythroid cells in the spleen started to decrease between PID 5 and 7 in the CB6F₁ mice that had been immunized once with peptide i. Virus-neutralizing antibodies in the serum were not detectable at PID 7 in FV-infected CB6F₁ mice regardless of whether they had been immunized with peptide i or not (Fig. 1d). In the CB6F₁ mice immunized with peptide i, virus-neutralizing IgM became detectable by PID 14, and the antibodies switched to IgG between PID 14 and 21. In the unimmunized mice, however, virus-neutralizing antibodies became detectable at PID 21, a week later than in

the peptide-immunized mice, and they did not switch to IgG even at PID 28. These results indicated that the FV-induced expansion of erythroid cells was prevented in the peptide-immunized mice before virus-neutralizing antibodies became detectable in the serum.

Protection against FV disease correlates with CD4⁺ T cell stimulation

To identify the minimal effective sequence of the peptide vaccine, a series of truncated peptides were compared for their *in vitro* T cell-stimulating and *in vivo* protection efficacies (Fig. 2b and c). It was clear that the C-terminal Arg residue was indispensable for the recognition of this epitope by T cells. In fact, a 17-mer peptide, i-R, that lacked only the C-terminal

Arg totally lost the ability to stimulate CD4⁺ T cell proliferation *in vitro*, while another 17-mer, *i*₁₇, that retained the Arg residue but lacked the N-terminal His kept the ability, albeit less efficiently than peptide *i*, to stimulate the T cells. When N-terminal residues were further removed from the 18-mer *i* and their efficacy to stimulate the CD4⁺ T cells was examined through the range of concentrations between 0.01 and 20 μM, the 13-mer (*i*₁₃) retained the T cell-stimulating activity and showed a stimulatory effect comparable to peptide *i*₁₇, while the 12-mer (*i*₁₂) showed a stimulatory effect <1/24 of that of the full-length peptide *i*. Peptide *i*₁₁ did not induce significant proliferation even when as much as 20 μM was added to the culture. In line with this result, the 13-mer retained the ability to induce protection against FV challenge in immunized CB6F₁ mice, while the 12-mer did not protect the same strain of mice against FV-induced disease even when five times more molecules were administered (Fig. 2c).

The requirement of CD4⁺ T cells for the peptide-induced immune protection was further confirmed by depleting CD4⁺ T cells from vaccinated CB6F₁ mice. The adopted schedule of the antibody administration resulted in undetectable CD4⁺ T cells in the spleen in separately examined uninfected animals for a period equivalent to PID 0–14, and lack of CD4⁺ T cells in the peripheral blood was confirmed in the vaccinated and infected group on PID 3–13 (data not shown). Antibody-induced depletion of CD4⁺ T cells abrogated the efficacy of peptide immunization, and CD4⁺ T cell-depleted animals died even more rapidly than the unimmunized control mice ($P < 0.05$). Injection of the control rat IgG did not affect the protective efficacy of the peptide vaccine, and ~80% of the peptide-immunized CB6F₁ mice that had been given the control antibody survived past PID 60 (Fig. 2d).

Peptide-induced immune protection against FV-induced disease in CB6F₁ mice genetically lacking a single component of the immune system

To examine possible effectiveness of the peptide immunization in mice genetically lacking either CD8⁺ T or B cell components of the immune system, we produced CB6F₁ mice with a homozygous disruption of the β_2m gene or of the Ig μ -chain gene. The absence of CD8⁺ T or B lymphocytes, respectively, was confirmed by flow cytometric analyses of the spleen and PBMCs (data not shown). In accordance with the prior experiments (Figs 1 and 2), $\geq 80\%$ of the wild-type CB6F₁ mice were protected against FV infection when immunized with peptide *i*. Protective efficacy of the 13-mer peptide, *i*₁₃, was further confirmed, and the development of early splenomegaly was prevented in 70% of the CB6F₁ mice given *i*₁₃ (Fig. 3a). Surprisingly, when CB6F₁- $\beta_2m^{-/-}$ mice lacking CD8⁺ T cells were immunized with peptide *i*, only <30% of the immunized mice developed splenomegaly and >70% survived until PID 100 in repeated experiments (Fig. 3). The observed survival curves were not significantly different between the peptide-immunized wild-type and $\beta_2m^{-/-}$ groups ($P > 0.4$), indicating a similar effectiveness of the peptide vaccine both in the presence and absence of CD8⁺ T cells. On the other hand, when the mice of the same susceptible CB6F₁ background that lacked B cells due to the homozygous μMT mutation were immunized with peptide *i*, they developed

splenomegaly and all died by PID 100, indicating crucial roles of B cells for the peptide-induced immune protection. Interestingly, however, the temporal changes in the incidences of splenomegaly and leukemic death delayed significantly in repeated experiments in the peptide-immunized, B cell-deficient mice compared with those in the unimmunized control mice of the same deficiency (Fig. 3c and f). The delay in the development of splenomegaly in the peptide-immunized $\mu MT/\mu MT$ mice was also substantiated by flow cytometric enumerations of FV-infected erythroid cells: at PID 7, $28.2 \pm 3.7\%$ ($n = 5$) of the nucleated spleen cells were positive for both TER-119 and F-MuLV gp70 in the unimmunized control mice, while the proportion of the TER-119⁺, gp70⁺ cells in the spleen was significantly smaller ($P < 0.05$) $12.1 \pm 8.2\%$ ($n = 5$) in the peptide-immunized $\mu MT/\mu MT$ mice. The effect of peptide immunization was more striking in the bone marrow where the percentage of TER-119⁺, gp70⁺ cells in the unimmunized mice was $11.1 \pm 4.4\%$, while that of the peptide-immunized mice was $0.72 \pm 0.22\%$ ($P < 0.03$) at PID 7. These results indicate some functions of non-B cells in delaying the FV-induced disease development.

Elimination of FV-producing cells from the spleen and bone marrow in the $\beta_2m^{-/-}$ mice immunized with peptide *i*

We next compared the numbers of FV-infected cells between peptide-immunized and unimmunized control mice using infectious center assays. The relative ratio in the number of FV-producing cells in the spleen between the peptide-immunized and unimmunized mice started to decrease at PID 8 as observed in the previous experiments (13, 14), and FV infectious centers became undetectable by our assays by PID 28 in peptide-immunized wild-type mice (Fig. 4a). The lack of detectable FV-producing cells in the spleen of all the tested, peptide-immunized CB6F₁ mice was confirmed by seeding the cells prepared from the entire spleen ($>10^8$) of each animal as infectious centers at PID 28. The number of FV-producing cells in the bone marrow was also significantly lower in the peptide-immunized wild-type mice than in the unimmunized control mice at PID 8, 14 and 21, and became undetectable at PID 28 (Fig. 4d). At PID 28, 2.1×10^7 bone marrow cells were tested from each mouse and no infectious centers were detectable by our assays in any of the examined animals. In the CB6F₁- $\beta_2m^{-/-}$ mice, the numbers of FV-producing cells in the spleen and bone marrow were significantly lower in the peptide-immunized than in unimmunized control mice at PID 14 and 28 (Fig. 4b and e), in accordance with the observed effectiveness of the peptide immunization in preventing the FV-induced disease development in the absence of CD8⁺ T cells (Fig. 3). It should be noted that in seven of the nine immunized animals tested at PID 28 no infectious centers were detectable even when the cells of the entire spleen were inoculated into the culture. However, there were also individuals among the peptide-immunized $\beta_2m^{-/-}$ mice in which FV-producing cells were still detectable in the spleen or bone marrow at PID 28 (Fig. 4b and e), while such cells were not detectable in any of the immunized wild-type mice tested at the same time point. These results imply that CD8⁺ T cells were not necessarily required but may play some roles in the elimination of virus-infected cells in peptide-immunized CB6F₁ mice.

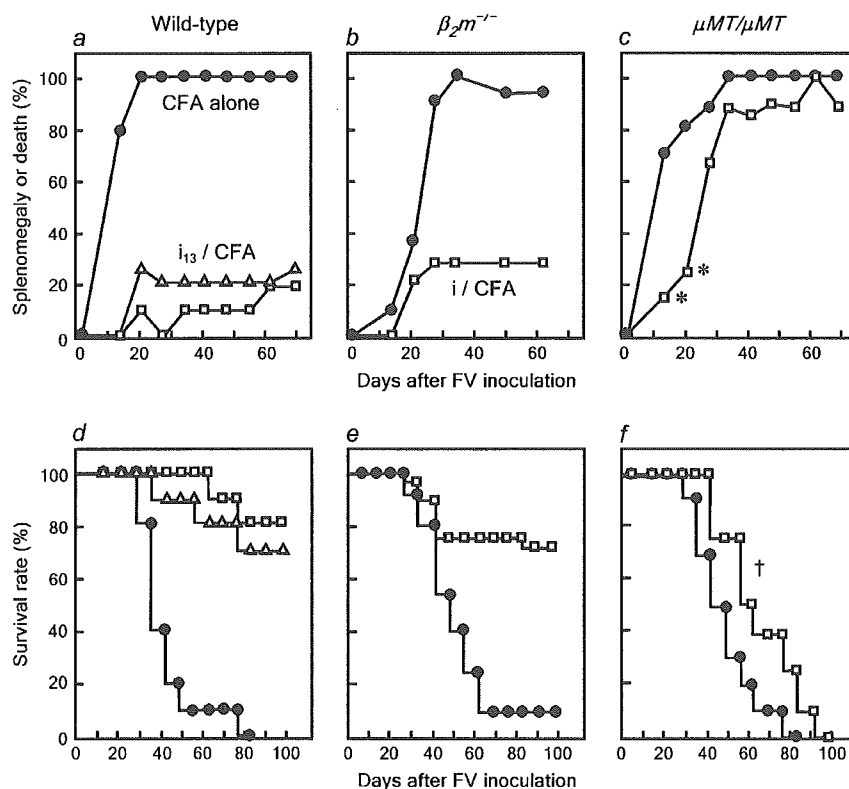


Fig. 3. Effects of immunization with peptide i on the development of FV-induced disease in CB6F₁ mice lacking CD8⁺ T or B cells. Wild-type CB6F₁ mice (a and d), CB6F₁ mice lacking CD8⁺ T cells due to homozygous targeting of the β_2m gene (b and e) and CB6F₁ mice lacking B cells due to homozygous targeting of the membrane exon of Ig μ -chain gene (c and f) were either immunized with 10 μ g per mouse of peptide i in CFA (\square) or given CFA alone (\bullet). Another group of the wild-type mice were immunized with 10 μ g per mouse of peptide i_{13} in CFA (Δ). Four weeks later, they were inoculated with 150 SFFV FV and followed for the development of splenomegaly and leukemic death. In (c), * indicates significant differences in the frequency of splenomegaly between the immunized and control groups ($P < 0.001$), and in (f), † indicates significant difference between the two survival curves ($P = 0.041$). The number of animals in each group were: (a) and (d), \square , 10; Δ , 10; \bullet , 10; (b) and (e), \square , 23; \bullet , 20 and (c) and (f), \square , 12; \bullet , 16. The experiments were performed twice with essentially identical results.

In accordance with the lack of protection against FV-induced disease development, virus-producing cells constantly increased between PID 5 and 21 in the spleen and bone marrow of the CB6F₁- μ MT/ μ MT mice, regardless of whether the hosts were immunized with peptide i or not. Interestingly, however, the numbers of virus-producing cells both in the spleen and bone marrow were significantly lower in the peptide-immunized, B cell-deficient mice than those in the unimmunized control mice of the same deficiency at PID 8 (Fig. 4f). This observation is consistent with the significant delay in the development of early splenomegaly and leukemic death (Fig. 3), and smaller numbers of TER-119⁺ and viral gp70⁺ FV-infected erythroid cells in the spleen and bone marrow in peptide-immunized, B cell-deficient CB6F₁ mice.

Priming and re-activation of CD4⁺ T cells in the peptide-immunized μ MT/ μ MT mice

To examine the possibility that the observed inefficiency in anti-FV protection of the immunization with peptide i in CB6F₁- μ MT/ μ MT mice might be due to the lack of APC activity, rather than antibody-producing function, of B lymphocytes, peptide-

specific proliferative responses were compared between the wild-type and μ MT/ μ MT animals. When CD4⁺ T cells purified from the wild-type CB6F₁ mice previously immunized with peptide i were used as responders, irradiated spleen cells both from the wild-type and from the μ MT/ μ MT animals induced strong proliferative responses, although the peptide-specific proliferation was significantly weaker when μ MT/ μ MT instead of the wild-type spleen cells were used as APC (Fig. 5a). FV infection significantly affected the APC function of wild-type spleen cells, but that of μ MT/ μ MT spleen cells was not significantly reduced when used at PID 10. Similar results were observed when CD4⁺ T cells purified from immunized μ MT/ μ MT animals were used as responders. Thus, CD4⁺ T cells were primed with peptide i in the absence of B cells, and spleen cells from μ MT/ μ MT animals could present the peptide antigen to primed CD4⁺ T cells, albeit less efficiently than the wild-type spleen cells, even after FV infection. Successful priming of CD4⁺ T cells and their re-activation upon FV infection in μ MT/ μ MT animals were further confirmed *in vivo* by analyzing the expression of an early activation marker, CD69, on T cells. Upon FV infection of peptide-immunized CB6F₁- μ MT/ μ MT

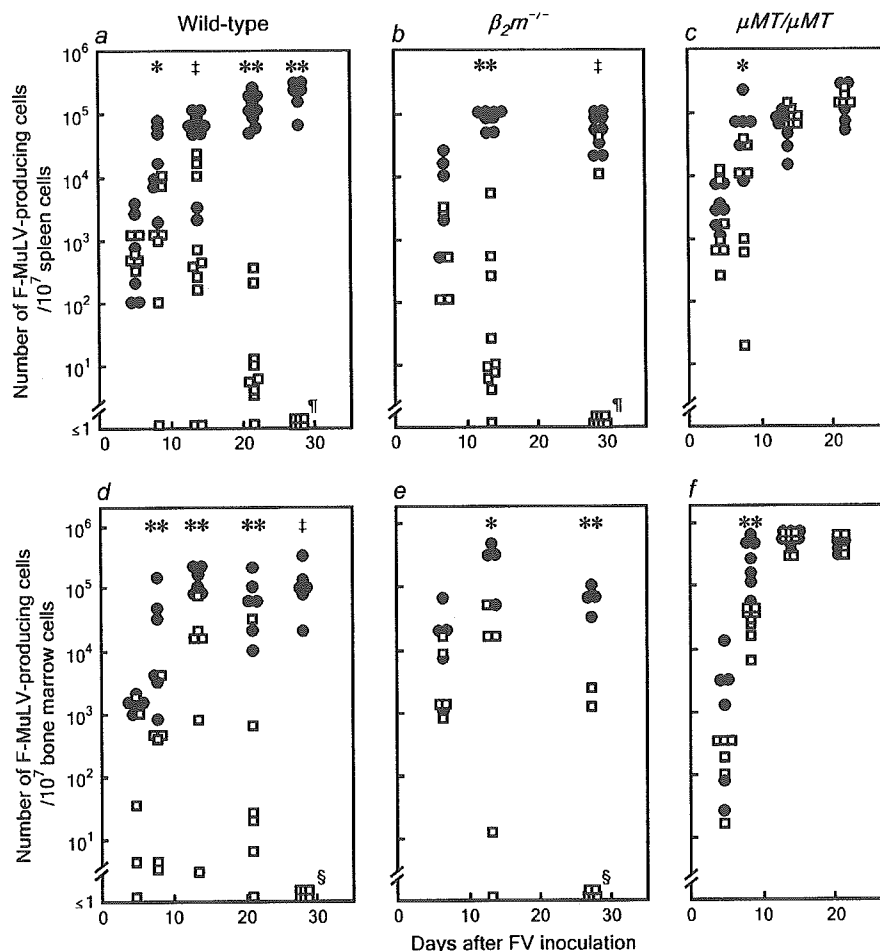


Fig. 4. Effects of immunization with peptide i on the number of FV-producing cells in CB6F₁ mice lacking CD8⁺ T or B cells. Wild-type CB6F₁ mice (a and d), the CB6F₁ mice lacking CD8⁺ T cells (b and e) and the CB6F₁ mice lacking B cells (c and f) were either immunized with 10 μ g per mouse of peptide i in CFA (\square) or given CFA alone (\bullet). Four weeks later, they were inoculated with 150 SFFV FV and FV-producing infectious centers were enumerated in the spleen (a–c) and bone marrow (d–f). Each data point shows the actual number of infectious centers detected from each individual mouse. At least 10^7 spleen and bone marrow cells were tested from each animal. At PID 28, the cells prepared from the entire spleen ($>10^8$, ¶) and 2.1×10^7 (from wild-type mice) or 3.1×10^7 (from $\beta_2m^{-/-}$ mice) bone marrow cells (§) were inoculated as infectious centers to ensure the lack of detectable virus-producing cells. Infectious centers were undetectable from any of the tested animals indicated with ¶ or § at PID 28. Statistical significance of the difference between the immunized and unimmunized groups at each time point was examined: * $P < 0.04$; ** $0.001 < P < 0.01$; ‡, $0.0002 < P < 0.001$.

mice, an increase in the proportion of CD69⁺ cells among CD4⁺ T cells was readily detectable (Fig. 5b). The percentages of CD69⁺ cells among CD4⁺ T cells in the spleen at PID 7 were significantly higher in the peptide-immunized than in the unimmunized animals, indicating re-activation of peptide-primed T cells upon FV infection (Fig. 5c). The effect of peptide immunization on the induction of CD69 expression was even more pronounced when bone marrow cells were tested (Fig. 5d). Interestingly, the CD69⁺ population among CD8⁺ T cells also showed a significant increase when peptide-immunized and unimmunized μ MT/ μ MT mice were compared at PID 7, confirming the previously demonstrated activation of CD8⁺ cytotoxic cells at PID 7 (14).

Production and class switching of serum antibodies reactive to the surface of FV-induced leukemia cells in the peptide-immunized mice

Although virus-neutralizing antibodies were not detectable in FV-infected animals until PID 14 (Fig. 1d), non-neutralizing anti-FV antibodies might have been produced at earlier time points, and might have contributed to the observed decrease in the number of FV-infected cells in the vaccinated animals, which was evident as early as PID 7 (Figs 1c and 4). Thus, the possible presence of anti-FV antibody in the serum was examined using FV-induced leukemia cells as indicators. The hemisynthetic ($H2^{bl/b}$), FV-induced leukemia cells Y57-2C expressed both the F-MuLV *gag* and *env* gene products as

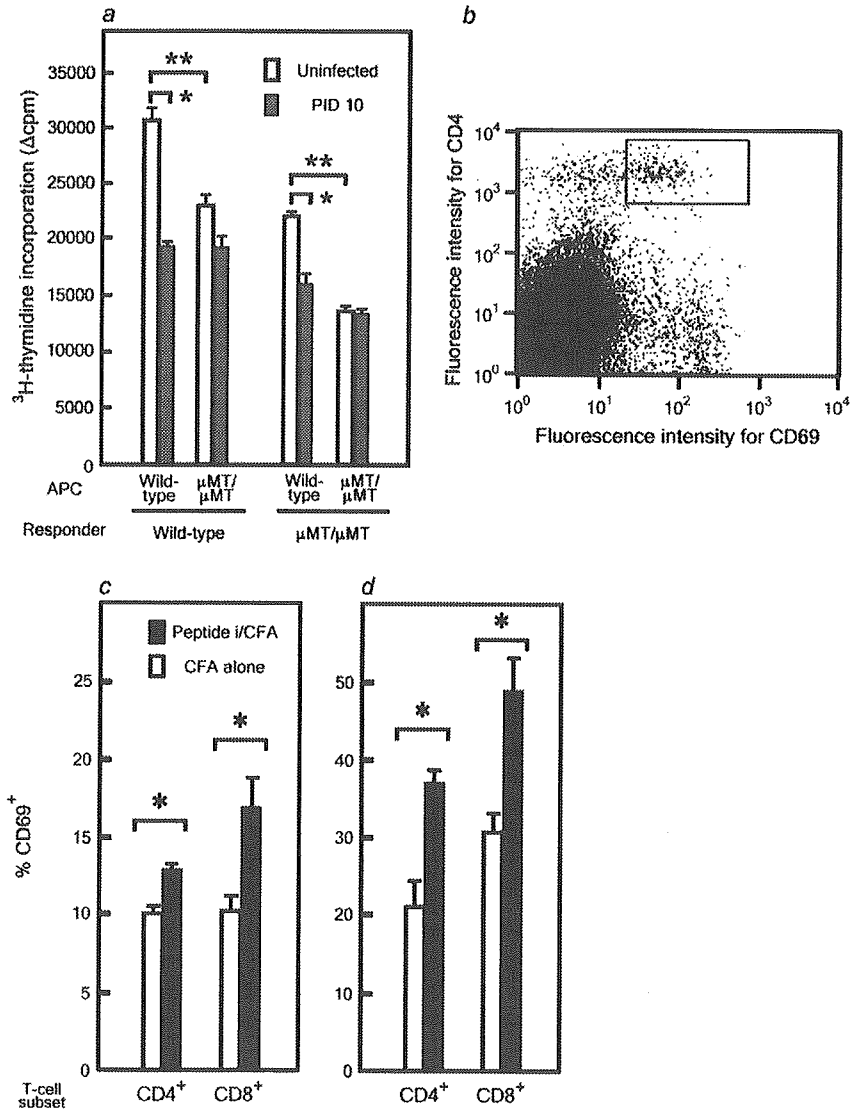


Fig. 5. Priming and re-activation of CD4⁺ T cells with peptide i in the B cell-deficient mice. (a) CD4⁺ T cells were purified from the spleen of wild-type and homozygous μ MT/ μ MT CB6F₁ mice at 3 weeks after a single immunization with 10 μ g per mouse peptide i emulsified in CFA. Proliferative responses were measured at 2 days after stimulation with 1 μ M peptide i along with the indicated APC. Spleen cells as APC were prepared from the wild-type and μ MT/ μ MT CB6F₁ mice either without FV inoculation or at PID 10, and γ -irradiated. The magnitude of antigen-specific proliferation is shown by Δ counts per minute (c.p.m.) in this chart by subtracting the average [³H]thymidine ([³H]TdR) incorporation into the cultures containing no peptide from that in the peptide-containing cultures. Levels of [³H]TdR incorporation into the cultures without a peptide were <120 c.p.m. Data shown are averages + SEM of triplicate cultures, and the experiments were performed twice with essentially the same results. *, significantly different at $P < 0.01$; ** $P < 0.001$. (b) A representative pattern of CD69 expression on CD4⁺ T cells in the bone marrow of the μ MT/ μ MT mice previously immunized with peptide i. The small rectangle indicates the gate used to calculate the percentage of CD69⁺ cells among CD4⁺ T cells. (c) and (d) Comparison of the percentages of CD69⁺ activated cells among CD4⁺ and CD8⁺ T cells in the spleen (c) and bone marrow (d) at 7 days after FV inoculation between the peptide-immunized and unimmunized μ MT/ μ MT mice. Data are averages + SEM calculated with five mice per group. *, the percentage of CD69⁺ population is significantly higher in the immunized than in the unimmunized mice at $P < 0.005$.

well as SFFV gp55 on their surfaces (Fig. 6a). Sera from FV-infected CB6F₁ mice bound onto the surface of Y57-2C cells, and geometric means of the fluorescence intensities decreased in proportion to serum dilutions (Fig. 6b). Therefore, at each time point titers of serum antibodies reactive to the surface of the FV-induced leukemia cells, designated

hereinafter anti-leukemia cell antibody titers, were determined by dividing geometric means of fluorescence intensities obtained by incubating the indicator cells with a 1/16 dilution of serum samples by the geometric mean of fluorescence intensities obtained with the same dilution of pooled control serum collected from uninfected CB6F₁ mice. Interestingly,

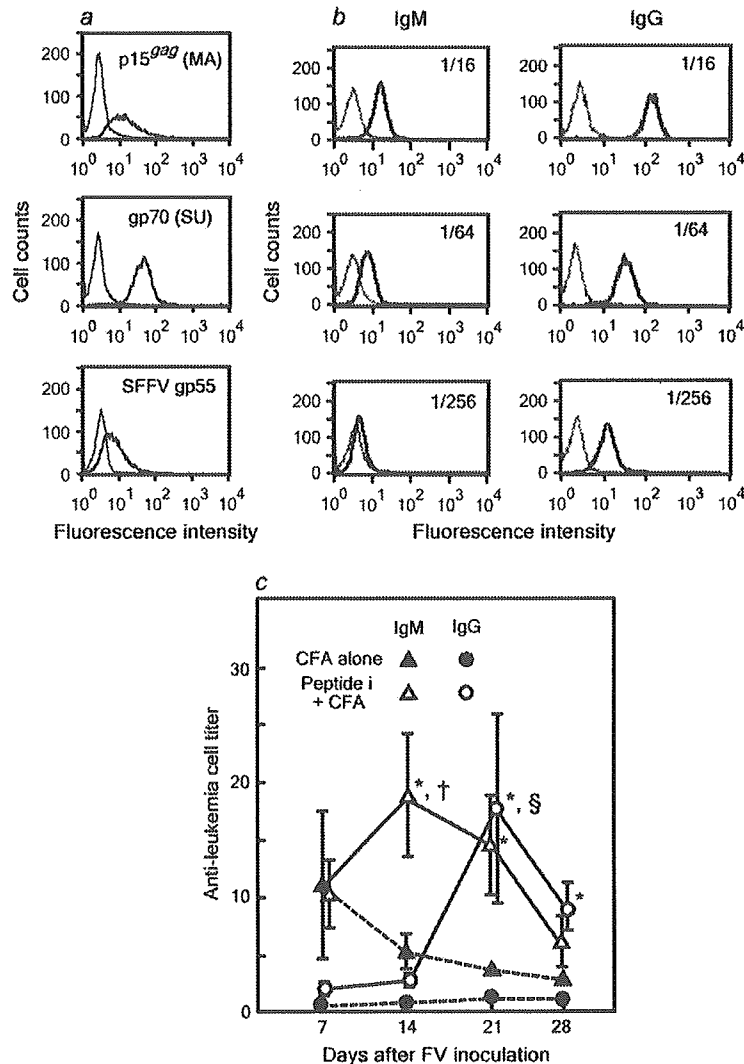


Fig. 6. Detection of serum antibody reactive to the surfaces of FV-induced leukemia cells in FV-infected CB6F₁ mice. (a) Expression of FV antigens on the surfaces of Y57-2C cells used as the indicators for FACS analyses. Thick lines represent the binding of each mAb reactive to the indicated FV gene product, while thin lines represent the binding of each isotype-matched control antibody. (b) Representative patterns showing the binding of serum IgM and IgG onto Y57-2C cells. A serum sample obtained from a peptide-immunized CB6F₁ mouse at PID 21 was diluted serially and incubated with Y57-2C cells. FACS patterns of IgM and IgG binding at the indicated serum dilution are shown, with thin lines representing the binding of the pooled control serum prepared from uninfected CB6F₁ mice at the same indicated dilution. Similar results were obtained when H2^{9/a} AA-41 leukemia cells were used as indicator cells. (c) Changes in the titers of IgM and IgG anti-leukemia cell antibodies detectable in the sera of CB6F₁ mice after FV infection. CB6F₁ mice were either immunized once with 10 µg per mouse peptide i in CFA or given CFA alone and challenged with 150 SFFU FV 4 weeks later. Each data point shows mean ± SEM calculated by using five to six mice per group. *, titers in the immunized mice are significantly higher than those in unimmunized mice at $P < 0.05$; †, the IgM titer is significantly higher than IgG titer at $P < 0.05$; §, the average IgG titer at PID 21 is significantly higher than that at PID 14, $P < 0.01$.

serum anti-leukemia cell antibodies were detectable as early as PID 7, but average titers of these antibodies decreased in the following 3 weeks of infection, and no class switching to IgG was observed in the unimmunized animals (Fig. 6c). In contrast, anti-leukemia cell IgM titers were significantly higher in the peptide-immunized than in the unimmunized control mice at PID 14, and IgG class of anti-

leukemia cell antibodies were detectable at PID 21 and 28 in the peptide-immunized animals.

Role of CD8⁺ T cells in the induction of Ig class switching of virus-neutralizing and anti-leukemia cell antibodies

Kinetics of the production and class switching of virus-neutralizing and anti-leukemia cell antibodies in the genetically

modified animals were analyzed between PID 7 and 28. Serum titers of FV-neutralizing IgM and IgG in unimmunized $\beta_2m^{-/-}$ mice were not significantly different from those in the unimmunized wild-type mice (compare Figs 1d and 7a). As in the case of peptide-immunized wild-type mice, production of virus-neutralizing IgM was detected at PID 14 in the serum of peptide-immunized $\beta_2m^{-/-}$ mice genetically lacking CD8⁺ T cells. However, in contrast to the peptide-immunized wild-type mice, neutralizing IgG titers in the peptide-immunized $\beta_2m^{-/-}$ animals were not significantly higher than their IgM titers even at PID 28, suggesting some roles of CD8⁺ T cells in facilitating class switching of virus-neutralizing antibodies in FV-infected mice. The role of CD8⁺ T cells in the induction of IgG class virus-neutralizing antibodies was further confirmed by transferring purified CD8⁺ T cells from peptide-immunized to unimmunized mice. Unimmunized mice did not possess detectable levels of virus-neutralizing antibodies in their serum at PID 10, and the antibodies were IgM-dominant at PID 20 (Fig. 7b), confirming the results of the kinetic analyses shown in Fig. 1(d). As expected, the recipients of CD4⁺ T cells from the peptide-immunized and FV-infected mice showed the

production of neutralizing IgG at PID 20. Interestingly, the recipients of highly purified CD8⁺ T cells from peptide-immunized and challenged mice also showed the production of virus-neutralizing IgG, the level of which was comparable to that in the recipients of the CD4⁺ T cell transfer. As controls, transfer of purified CD4⁺ or CD8⁺ T cells from unimmunized control mice into FV-infected CB6F₁ mice did not induce significant class switching of virus-neutralizing antibodies even at PID 20 (data not shown). No neutralizing antibodies were detectable in FV-infected $\mu MT/\mu MT$ mice regardless of whether they were immunized with peptide i or not.

When anti-leukemia cell antibodies in the sera were tested, unimmunized $\beta_2m^{-/-}$ mice possessed anti-leukemia cell IgM at PID 7 and their titers decreased toward PID 14 as observed in the unimmunized wild-type mice (Fig. 7c). High titers of anti-leukemia cell IgM were also detectable in the peptide-immunized $\beta_2m^{-/-}$ mice at PID 7; however, in contrast to the peptide-immunized wild-type mice, $\beta_2m^{-/-}$ mice did not show a significant increase in the IgG titers between PID 14 and 21, confirming inefficient class switching of both neutralizing and anti-leukemia cell antibodies in the $\beta_2m^{-/-}$ animals.

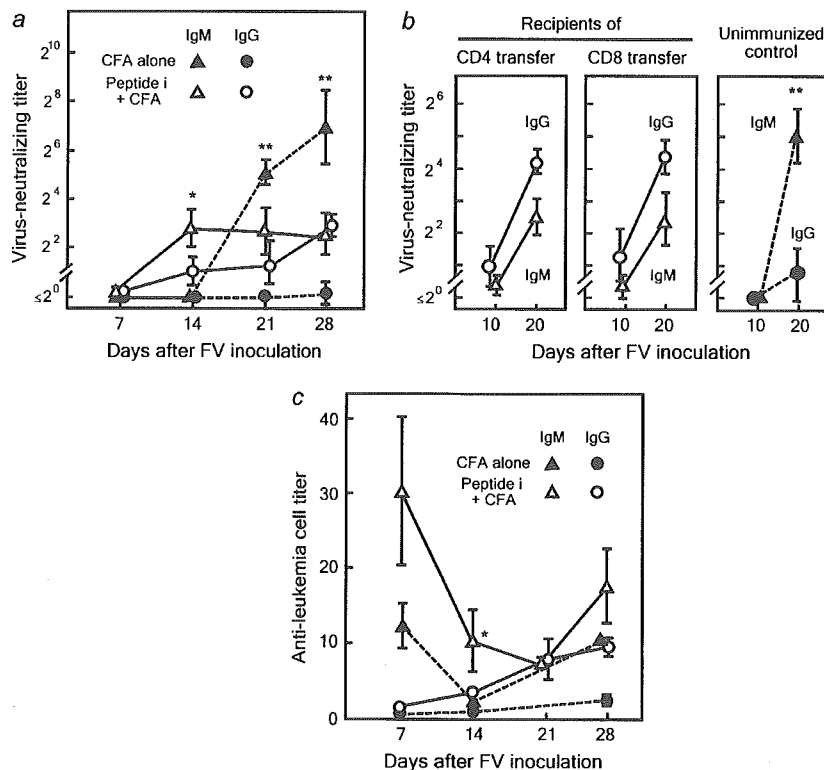


Fig. 7. Titers of virus-neutralizing and anti-leukemia cell IgM and IgG antibodies in sera from the CD8⁺ T cell-deficient CB6F₁ mice and the effect of immune T cell transfer on the production of virus-neutralizing antibody. (a) CB6F₁- $\beta_2m^{-/-}$ mice were either immunized with peptide i or given CFA alone and challenged with FV as described. Sera were collected at the indicated time points and their neutralizing IgM and IgG titers were determined. Each data shows mean \pm SEM calculated from five to nine serum samples, with statistically significant differences between the paired IgG and IgM titers indicated with * $P < 0.03$; ** $P < 0.001$. (b) CD4⁺ and CD8⁺ T cells were purified from the spleen of peptide-immunized CB6F₁ mice at PID 7 and separately transferred into unimmunized control mice at PID 7. Sera were collected 3 (PID 10) and 13 days (PID 20) after cell transfer. Data shown here are mean \pm SEM calculated from 4 to 5 serum samples at each time point. Differences between neutralizing IgM and IgG titers were compared by paired t -test: ** $P < 0.005$. (c) Changes in the titers of IgM and IgG anti-leukemia cell antibodies detectable in the sera after FV infection. Each data point shows mean \pm SEM calculated by using four to seven mice per group. *, the indicated titer in the immunized mice is significantly higher than that in unimmunized mice at $P < 0.05$.

Discussion

In the present study, we attempted to unravel the different roles of CD8⁺ T and B cells in peptide-induced immune protection against FV-induced disease development by using genetically modified animals of the highly susceptible CB6F₁ background. CB6F₁ mice immunized only once with the peptide that contained a single CD4⁺ T cell epitope were protected against fatal FV disease, and the development of early erythroid cell proliferation was prevented by the peptide immunization. The minimum sequence of the peptide required for *in vivo* protection against FV challenge, VYSQFEKSYRHKR, was the same as that required for CD4⁺ T cell stimulation *in vitro*, indicating a close correlation between the peptide's ability to stimulate CD4⁺ T cells and its efficacy in inducing protective immunity against FV-induced disease development. The requirement of CD4⁺ T cells for the peptide-induced immune protection against FV infection was further confirmed by the lack of protection in the vaccinated animals after antibody-induced depletion of CD4⁺ T cells.

In contrast to the bursting of TER-119⁺ erythroid cells in the spleen of the unimmunized mice starting from PID 7, the reduction in the number of erythroid cells was observed between PID 5 and 7 in the peptide-immunized CB6F₁ mice, before virus-neutralizing antibodies became detectable in the serum (Fig. 1), and the numbers of spleen and bone marrow infectious centers were significantly smaller in the immunized than in the unimmunized control mice at PID 8 (Fig. 4). Although IgM antibodies reactive to the surfaces of FV-induced leukemia cells were detectable at as early as PID 7 (Figs 6 and 7), these antibodies are unlikely to play major roles in the observed suppression of the early growth of FV-infected cells in the vaccinated animals because anti-leukemia cell titers were not significantly different between the immunized and unimmunized groups at PID 7 (Fig. 6). This notion is consistent with the significantly reduced numbers, in comparison with those in unimmunized animals, of infectious centers in the spleen and bone marrow of the vaccinated mice at PID 8 even in the absence of B cells (Fig. 4c and f), and suggests the possibility that cellular immune responses, rather than antibodies, are involved in the regulation of SFFV-induced erythroid cell proliferation. In this regard, significantly larger populations of both CD4⁺ and CD8⁺ T cells were activated in the peptide-immunized, B cell-deficient mice in comparison with those in the unimmunized control mice at PID 7 (Fig. 5), and cytotoxic effector functions exerted by CD4⁺ and CD8⁺ T cells and those exerted more efficiently by NK cells have been demonstrated at as early as PID 7 in FV-infected CB6F₁ mice (14). These non-B effector cells might be involved in the control of SFFV-induced erythroid cell proliferation through direct killing of infected target cells. On the other hand, the numbers of virus-producing cells detected after PID 14 in the spleen and bone marrow were not different between the immunized and unimmunized groups of the B cell-deficient mice (Fig. 4c and f). This is again consistent with the detection of significantly higher titers of virus-neutralizing and anti-leukemia cell antibodies in the serum of vaccinated than in the unimmunized wild-type and $\beta_2m^{-/-}$ animals starting from PID 14 (Figs 1d, 6 and 7). These data suggest that the observed elimination of FV-producing cells in the peptide-immunized

mice after PID 14 may depend mainly on the production of antibodies. Thus, early prevention of erythroid cell proliferation apparently depends mainly on cellular immune responses, but humoral responses seem to play crucial roles in the elimination of virus-producing cells in the later stage.

As to the relationship and relative importance between virus-neutralizing and anti-leukemia cell antibodies, tempos of the production and class switching of these antibodies after PID 14 were similar in the vaccinated wild-type animals (Figs 1d and 6c). However, in unimmunized animals, significant production of virus-neutralizing IgM was detectable after PID 21 when anti-leukemia cell titers were low and diminishing. Similarly, paradoxical production of virus-neutralizing antibodies in the presence of low anti-leukemia cell antibody titers has been observed in $H2^{alb}$ (A.BY \times A/WySn)F₁ mice at 20 days after FV infection (Miyazawa, M., Ishihara, C., and Takei, Y. A., unpublished results). It should be noted that although the anti-leukemia cell IgM titers at PID 21 and 28 were low, mean fluorescence intensities were four to five times higher than that obtained with the control serum, which reflects significant shifting of the peaks of fluorescence (Fig. 6b). Thus, it is conceivable that only a small proportion of serum antibodies detectable as anti-leukemia cell antibodies exhibit virus-neutralizing capability especially in the early stage of FV infection, and the proportion of neutralizing antibodies among anti-FV antibodies increases in the later stage. This interpretation also suggests that the production of antibodies reactive to virus-neutralizing epitopes, but not just any anti-FV antibody, depends on T cells. Further studies are required to elucidate the molecular and epitope specificities of neutralizing and anti-leukemia cell antibodies. It can be pointed out that the presence of virus-neutralizing IgM at PID 21 is not effective to reduce the number of FV-infected cells as clearly shown in the case of unimmunized, wild-type CB6F₁ mice (Figs 1d and 4). Further, class switching to IgG of virus-neutralizing and anti-leukemia cell antibodies may not be a requisite because the number of FV infectious centers were reduced in the absence of efficient class switching in the peptide-immunized $\beta_2m^{-/-}$ mice (Figs 4 and 7). Thus, the presence of virus-neutralizing and/or anti-leukemia cell IgM at around PID 14 might be crucial in preventing the spread of FV infection to a large enough number of target cells to support progressive infection.

Using partially FV-resistant (B10.A \times A.BY)F₁ mice and an N-tropic F-MuLV as an attenuated vaccine, Dittmer, Brooks, and Hasenkrug (11) dissected different roles of the immune cell components in protection against FV-induced disease development. Their demonstration of the effectiveness in inducing the recovery from initial splenomegaly of cell transfer from vaccinated to naive animals after depletion of immune CD8⁺ T cells is in agreement with our results showing the peptide-induced reduction of FV-producing cells in the spleen and bone marrow in the absence of CD8⁺ T cells (Fig. 4). However, the development of splenomegaly was prevented only when the whole spleen cells or all three sub-populations (CD4⁺, CD8⁺ and CD19⁺) of lymphocytes were transferred from the vaccinated to naive animals in the above live vaccine experiments, while in the present study the development of early splenomegaly was prevented in >70% of the CB6F₁- $\beta_2m^{-/-}$ mice after immunization with peptide i. This apparent discrepancy may be due to the difference in challenge dose of

FV (10 000 versus 150 SFFU), or might also be explained by the exaggerated and earlier production of IFN- γ from CD4⁺ T cells and persistent activation of NK cells in $\beta_2m^{-/-}$ mice in comparison with those in their wild-type counterparts (30), as discussed below.

Dittmer, Brooks, and Hasenkrug (11) also showed that passive immunization with a virus-neutralizing mAb prior to FV challenge resulted in a significant reduction in the number of virus-producing cells at PID 10 and recovery from the initial development of splenomegaly, although 2.9×10^6 infectious centers on average were still detectable in the spleen. This result is partly consistent with our demonstration that B cells are required for the elimination of virus-producing cells from the spleen and bone marrow, especially after PID 14. However, the reported lack of protection after the transfer of B cells from vaccinated to naive mice contrasts with our demonstration of the crucial role of B cells. As they discussed later (12), transferred B cells might not have produced a sufficient level of FV-reactive antibodies until they were re-stimulated upon FV challenge of the recipients. In this regard, the production of virus-neutralizing antibodies in FV-infected mice is dependent on CD4⁺ T cells (31). Further, we have shown in our previous (13, 17) and the present experiments that peptide-induced priming of CD4⁺ T cells facilitates both production and class switching of virus-neutralizing and anti-leukemia cell antibodies upon FV infection. Thus, the lack of protection by the transfer of purified B cells alone from vaccinated to naive mice does not necessarily contradict our demonstration of the requirement of B cells for peptide-induced immune protection, especially because the titers of anti-FV antibody had not been determined in the above-reported B cell-transferred animals. The same authors (32) have shown that the presence of virus-neutralizing antibodies at the time of infection is crucial for a vaccine-induced protection of naturally resistant C57BL/6 mice against FV infection.

The observed lack of protection in the $\mu MT/\mu MT$ mice might also be caused by the lack of or inefficient priming and/or re-activation of CD4⁺ T cells due to the absence of B cells as APC. Although successful priming of CD4⁺ and CD8⁺ T cells with protein as well as cellular antigens and effective induction of CTL responses have been reported in the $\mu MT/\mu MT$ mice (33, 34), the effect of the homozygous μMT mutation on T cell priming can be variable (35). However, since we were using as immunogen the 18-mer peptide which has been shown to directly bind onto the MHC class II E^{b/d} molecule (23), the uptake and processing of the given antigen by B cells were not required. In such cases where already processed peptide is used as an immunogen, B cells are regarded as unnecessary for the priming of T cells (35). In fact, CD4⁺ cells purified from the peptide-immunized $\mu MT/\mu MT$ mice showed potent proliferative responses upon re-stimulation with peptide i, and larger numbers of CD4⁺ T cells were activated upon FV infection in the peptide-immunized than in the unimmunized B cell-deficient mice (Fig. 6). Thus, the $\mu MT/\mu MT$ mice were not protected most conceivably because they lacked antibody production.

In previous reports, CD8⁺ T cells have always been associated with spontaneous and vaccine-induced immune resistance against FV infection: antibody-induced depletion of CD8⁺ T cells abrogated spontaneous recovery from

FV-induced splenomegaly in highly resistant (C57BL/10 \times A.BY)_{F1} mice (9), and recovery from splenomegaly was induced by transferring purified CD8⁺ T cells from (B10.A \times A.BY)_{F1} mice previously vaccinated with the live N-tropic F-MuLV into naive animals (11). These results apparently contradict the present results showing successful protection of the $\beta_2m^{-/-}$ mice with the peptide vaccine. However, in the case of spontaneous recovery observed in the strain (C57BL/10 \times A.BY)_{F1}, CD4⁺ T cells were not primed prior to FV infection, and mice were infected with 1500 SFFU of B-tropic FV, a ten times higher dose than we used in the present study. Thus, infection-induced priming of CD4⁺ T cells might have been inefficient or too slow in inducing effector mechanisms other than CD8⁺ T cells, which might be required to confine the rapid spread of inoculated FV. In this regard, CD8⁺ T cells are required not solely as cytotoxic effector cells but are also involved in the generation of T helper type 1 cells in FV-infected mice (36, 37). Thus, antibody-induced depletion of CD8⁺ T cells quite likely had also affected CD4⁺ T cell functions in the experiment reported by Robertson *et al.* (9), and adoptive transfer of immune CD8⁺ cells must have induced the activation of CD4⁺ effector cells in the recipients in the experiment performed by Dittmer, Brooks, and Hasenkrug (11). The role of CD8⁺ T cells in inducing class switching of virus-neutralizing and anti-leukemia cell antibodies (Fig. 7) might reflect the reported influence of CD8⁺ T cells on helper functions of CD4⁺ T cells. In fact, the effect of CD8⁺ T cell transfer from vaccinated to naive animals along with passive immunization with the neutralizing mAb was dependent on the presence of endogenous CD4⁺ T cells in the recipients (11). Thus, the reported requirement of CD8⁺ T cells for spontaneous resistance and vaccine-induced protection against FV infection might be compensated, at least partly, by the peptide-induced priming of CD4⁺ T cells. It has been shown that the effect of CD8⁺ T cells on the induction of protective CD4⁺ T cell responses is blocked by neutralizing anti-IFN- γ antibody (37). Likewise, intravenous administration of neutralizing anti-IFN- γ antibody on the day of FV challenge and at PID 7 abrogated the effect of peptide vaccine in six of seven injected CB6F₁ mice in our preliminary experiment (data not shown). Thus, all these data indicate that the apparent requirement of CD8⁺ T cells for spontaneous resistance and observed effectiveness of CD8⁺ T cell transfer in vaccine-induced protection against FV infection might have been actually mediated through the effect of CD8⁺ T cells on CD4⁺ T cell functions, and peptide-induced priming of CD4⁺ T cells may have bypassed the CD8⁺ T cell functions and induced protection in the $\beta_2m^{-/-}$ mice.

Actual effector mechanisms involved in the observed elimination of FV-infected erythroid cells in the absence of CD8⁺ T cells (Fig. 4) may include the previously described CD4⁺ CTLs and NK cells (14), as well as FV-reactive, cytotoxic antibody (38). However, anti-leukemia cell IgMs were detectable in both immunized and unimmunized animals at PID 7 (Figs 6 and 7), excluding the role of these antibodies in controlling the growth of FV-infected cells in the early stage. It should be emphasized that killing activities of CD4⁺ cytotoxic and NK cells were detectable in the peptide-immunized CB6F₁ mice at as early as PID 7, and NK cells were much more efficient than CD8⁺ CTLs in killing FV-induced leukemia

cells (14). Further, it has been shown that activation of NK cells after lymphocytic choriomeningitis virus infection is prolonged in $\beta_2m^{-/-}$ mice than in the wild-type mice (30). Thus, similarly enhanced activation of NK cells, along with the exaggerated production of IFN- γ from vaccine-primed CD4⁺ T cells, might have compensated otherwise indispensable CD8⁺ T cell functions in the peptide-immunized CB6F₁- $\beta_2m^{-/-}$ mice. In this regard, the incidences of splenomegaly in unimmunized CB6F₁- $\beta_2m^{-/-}$ mice at PID 14 and 21 were significantly lower than those in the unimmunized wild-type mice ($P < 0.001$), although their survival curves were not significantly different ($P > 0.05$) (Fig. 4). These observations are consistent with the previously observed activation and killing efficacy of NK cells in FV-infected CB6F₁ mice without prior immunization (14), and with the reported enhancement of virus-induced NK cell activity in $\beta_2m^{-/-}$ mice (30).

Taken together, the present study has demonstrated that for efficient immune protection against FV infection with the single-epitope peptide, B cells are more important than CD8⁺ T cells, but B cell-independent responses, probably exerted by previously demonstrated CD4⁺ CTLs and NK cells, do play some roles in the earlier stage of FV-induced disease development in suppressing the expansion of FV-infected erythroid cells. Careful comparison of these results and other reports may suggest the possibility that priming of CD4⁺ T cells with the peptide vaccine might allow the bypassing of the CD8⁺ T cell functions that have been reported to induce CD4⁺ T_H1 effector cells. These observations may contribute to the development of efficient vaccine strategies against other virus infections.

Acknowledgements

This work was supported in part by grants from the Ministry of Education, Culture, Sports, Science and Technology of Japan including the High-Tech Research Center grant, those from the Ministry of Health, Labor and Welfare of Japan and those from the Japan Health Science Foundation. We are grateful to M. Patrick Gorman for critically reading and correcting the manuscript.

Abbreviations

7-AAD	7-aminoactinomycin D
APC	antigen-presenting cell
B6	C57BL/6
CB6F ₁	(BALB/c × C56BL/6)F ₁
ED ₅₀	dose required to induce 50% of the maximum response
FBS	fetal bovine serum
F-MuLV	Friend murine leukemia virus
FV	Friend retrovirus complex
β_2m	β_2 -microglobulin
μ MT	Ig μ -chain membrane exon-targeted
PBBS	phosphate-buffered balanced salt solution
PID	post-infection day
SFFU	spleen focus-forming unit
SFFV	spleen focus-forming virus

References

- Chesebro, B., Miyazawa, M. and Britt, W. J. 1990. Host genetic control of spontaneous and induced immunity to Friend murine retrovirus infection. *Annu. Rev. Immunol.* 8:477.
- Kabat, D. 1989. Molecular biology of Friend viral erythroleukemia. *Curr. Top. Microbiol. Immunol.* 148:1.
- Morrison, R. P., Nishio, J. and Chesebro, B. 1986. Influence of the murine MHC (H-2) on Friend leukemia virus-induced immunosuppression. *J. Exp. Med.* 163:301.
- Chesebro, B. and Wherly, K. 1979. Identification of a non-H-2 gene (*Rfv-3*) influencing recovery from viremia and leukemia induced by Friend virus complex. *Proc. Natl Acad. Sci. USA* 76:425.
- Miyazawa, M., Nishio, J., Wehrly, K. and Chesebro, B. 1992. Influence of MHC genes on spontaneous recovery from Friend retrovirus-induced leukemia. *J. Immunol.* 148:644.
- Hasenkrug, K. J., Valenzuela, A., Letts, V. A., Nishio, J., Chesebro, B. and Frankel, W. 1995. Chromosomal mapping of *Rfv3*, a host resistance gene to Friend mouse retrovirus. *J. Virol.* 69:2617.
- Super, H. J., Hasenkrug, K. J., Simmons, S. *et al.* 1999. Fine mapping of the Friend retrovirus resistance gene, *Rfv3*, on mouse chromosome 15. *J. Virol.* 73:7848.
- Kanari, Y., Clerici, M., Abe, H. *et al.* 2005. Genotypes at chromosome 22q12-13 are associated with HIV-1-exposed but uninfected status in Italians. *AIDS* 19:1015.
- Robertson, M. N., Spangrude, G. J., Hasenkrug, K. *et al.* 1992. Role and specificity of T-cell subsets in spontaneous recovery from Friend virus-induced leukemia in mice. *J. Virol.* 66:3271.
- Perry, L. L., Miyazawa, M., Hasenkrug, K., Wehrly, K., David, C. S. and Chesebro, B. 1994. Contrasting effects from a single major histocompatibility complex class II molecule (H-2E) in recovery from Friend virus leukemia. *J. Virol.* 68:4921.
- Dittmer, U., Brooks, D. M. and Hasenkrug, K. J. 1999. Requirement for multiple lymphocyte subsets in protection by a live attenuated vaccine against retroviral infection. *Nat. Med.* 5:189.
- Dittmer, U. and Hasenkrug, K. J. 2000. Different immunological requirement for protection against acute versus persistent Friend retrovirus infections. *Virology* 272:177.
- Miyazawa, M., Fujisawa, R., Ishihara, C. *et al.* 1995. Immunization with a single T helper cell epitope abrogates Friend virus-induced early erythroid proliferation and prevents late leukemia development. *J. Immunol.* 155:748.
- Iwanami, N., Niwa, A., Yasutomi, Y., Tabata, N. and Miyazawa, M. 2001. Role of natural killer cells in resistance against Friend retrovirus-induced leukemia. *J. Virol.* 75:3152.
- Earl, P. L., Moss, B., Morrison, R. P., Wherly, K., Nishio, J. and Chesebro, B. 1986. T-lymphocyte priming and protection against Friend leukemia virus by vaccine-retrovirus *env* gene recombinant. *Science* 234:728.
- Kitamura, D., Rose, J., Kühn, R. and Rajewski, K. 1991. A B cell-deficient mouse by targeted disruption of the membrane exon of the immunoglobulin μ chain gene. *Nature* 350:423.
- Sugahara, D., Tsuji-Kawahara, S. and Miyazawa, M. 2004. Identification of a protective CD4⁺ T-cell epitope in p15^{gag} of Friend murine leukemia virus and role of the MA protein targeting the plasma membrane in immunogenicity. *J. Virol.* 78:6322.
- Robertson, M. N., Miyazawa, M., Mori, S. *et al.* 1991. Production of monoclonal antibodies reactive with a denatured form of the Friend murine leukemia virus gp70 envelope protein: use in a focal infectivity assay, immunohistochemical studies, electron microscopy and Western blotting. *J. Virol. Methods* 34:255.
- Miyazawa, M., Nishio, J. and Chesebro, B. 1992. Protection against Friend retrovirus-induced leukemia by recombinant vaccinia viruses expressing the *gag* gene. *J. Virol.* 66:4497.
- Iwashiro, M., Kondo, T., Shimizu, T. *et al.* 1993. Multiplicity of virus-encoded helper T-cell epitopes expressed on FBL-3 tumor cells. *J. Virol.* 67:4533.
- Kondo, T., Uenishi, H., Shimizu, T. *et al.* 1995. A single retroviral gag precursor signal peptide recognized by FBL-3 tumor-specific cytotoxic T lymphocytes. *J. Virol.* 69:6735.
- Shimizu, T., Uenishi, H., Teramura, Y. *et al.* 1994. Fine specificity of a virus-encoded helper T-cell epitope expressed on FBL-3 tumor cells. *J. Virol.* 68:7704.
- Uenishi, H., Iwanami, N., Yamagishi, H. *et al.* 1998. Induction of cross-reactivity in an endogenous viral peptide non-reactive to FBL-3 tumor-specific helper T-cell clone. *Microbiol. Immunol.* 42:479.
- Sitbon, M., Sola, B., Evans, L. *et al.* 1986. Hemolytic anemia and erythroleukemia, two distinct pathogenic effects of Friend

198 Anti-retroviral protection in the absence of CD8⁺ T

- MuLV: mapping of the effects to different regions of the viral genome. *Cell* 47:851.
- 25 Hashimoto, K., Tabata, N., Fijisawa, R., Matsumura, H. and Miyazawa, M. 2000. Induction of microangiopathic thrombocytopenia in normal mice by transferring a platelet-reactive, monoclonal anti-gp70 autoantibody established from MRL/lpr mice: an autoimmune model of thrombotic thrombocytopenic purpura. *Clin. Exp. Immunol.* 119:47.
- 26 Schmid, I., Uittenbogaart, C. H., Keld, B. and Giorgi, J. V. 1994. A rapid method for measuring apoptosis and dual-color immunofluorescence by single laser flow cytometry. *J. Immunol. Methods* 170:145.
- 27 Kina, T., Ikuta, K., Takayama, E. *et al.* 2000. The monoclonal antibody TER-119 recognizes a molecule associated with glycoprotein A and specifically marks the late stages of murine erythroid lineage. *Br. J. Haematol.* 109:280.
- 28 Chesebro, B., Wehrly, K., Cloyd, M. *et al.* 1981. Characterization of mouse monoclonal antibodies specific for Friend murine leukemia virus-induced leukemia cells: Friend-specific and FMR-specific antigens. *Virology* 112:131.
- 29 Dialynas, D. P., Quan, Z. S., Wall, K. A. *et al.* 1983. Characterization of the murine T cell surface molecule, designated L3T4, identified by monoclonal antibody GK1.5: similarity of L3T4 to the human LEU-3/T4 molecule. *J. Immunol.* 131:2445.
- 30 Vikingsson, A., Pederson, K. and Muller, D. 1996. Altered kinetics of CD4⁺ T cell proliferation and interferon- γ production in the absence of CD8⁺ T lymphocytes in virus-infected β 2-microglobulin-deficient mice. *Cell. Immunol.* 173:261.
- 31 Super, H. J., Brooks, D., Hasenkrug, K. and Chesebro, B. 1998. Requirement for CD4⁺ T cells in the Friend murine retrovirus neutralizing antibody response: evidence for functional T cells in genetic low-recovery mice. *J. Virol.* 72:9400.
- 32 Messer, R. J., Dittmer, U., Peterson, K. E. and Hasenkrug, K. J. 2004. Essential role of virus-neutralizing antibodies in sterilizing immunity against Friend retrovirus infection. *Proc. Natl Acad. Sci. USA* 101:12260.
- 33 Asano, M. S. and Ahmed, R. 1996. CD8 T cell memory in B cell-deficient mice. *J. Exp. Med.* 183:2165.
- 34 Epstein, M. M., Di Rosa, F., Jankovic, D., Sher, A. and Matzinger, P. 1995. Successful T cell priming in B cell-deficient mice. *J. Exp. Med.* 182:915.
- 35 Rivera, A., Chen, C.-C., Ron, N., Dougherty, J. P. and Ron, Y. 2001. Role of B cells as antigen-presenting cells *in vivo* revisited: antigen-specific B cells are essential for T cell expansion in lymph nodes and for systemic T cells responses to low antigen concentrations. *Int. Immunol.* 13:1583.
- 36 Peterson, K. E., Iwashiro, M., Hasenkrug, K. J. and Chesebro, B. 2000. Major histocompatibility complex class I gene controls the generation of gamma interferon-producing CD4⁺ and CD8⁺ T cells important for recovery from Friend retrovirus-induced leukemia. *J. Virol.* 74:5363.
- 37 Peterson, K. E., Stromnes, I., Messer R., Hasenkrug, K. and Chesebro, B. 2002. Novel role of CD8⁺ T cells and major histocompatibility complex class I genes in the generation of protective CD4⁺ Th1 responses during retrovirus infection in mice. *J. Virol.* 76:7942.
- 38 Chesebro, B. and Wherly, K. 1976. Studies on the role of the host immune responses in recovery from Friend virus leukemia. I. Antiviral and antileukemia cell antibodies. *J. Exp. Med.* 143:73.

Yohei Kida · Sachiyo Tsuji-Kawahara
Valentina Ostapenko · Saori Kinoshita
Eiji Kajiwara · Hiroyuki Kawabata · Takae Yuasa
Iwao Nishide · Susumu Yukawa · Masakazu Ichinose
Masaaki Miyazawa

Increased liver temperature efficiently augments human cellular immune response: T-cell activation and possible monocyte translocation

Received: 4 August 2005 / Accepted: 25 January 2006
© Springer-Verlag 2006

Abstract Hyperthermia (HT), in combination with other conventional therapeutic modalities, has become a promising approach in cancer therapy. In addition to heat-induced apoptosis, an augmented immunological effect is considered to be a benefit of hyperthermic treatment over chemo- or radiotherapy. Here, we investigated the effect of regional HT targeting the liver on immune cells, especially T cells and antigen-presenting cells, which are important in recognizing and eliminating tumor cells and pathogens such as viruses. In healthy volunteers exposed to such regional HT, both CD4⁺ and CD8⁺ T cells that express an activation marker CD69 increased transiently at 1 h post-treatment, with a subsequent decrease to base levels at 6 h after the treatment. At 24 h post-treatment, the percentage of CD69-positive cells significantly increased again but only among CD8⁺ T cells. IFN- γ production from PHA-stimulated peripheral blood mononuclear cells was gradually and significantly increased in the 2 days following the heating procedure, peaking at 36 h post-treatment. Furthermore, we found marked increases in plasma levels of IL-1 β and IL-6 starting at 24 h post-treatment. With regard to the number of each leukocyte subpopulation, a transient and dramatic decrease in the number of a subset of monocytes, CD14⁺CD16⁻ cells, was observed at 1 h after the hyperthermic

treatment, suggesting that the regional HT aimed at the liver may have influenced the extravasation of blood monocytes. No significant changes in T-cell activities or monocyte counts were observed in the volunteers exposed to heating of the lungs or the legs. These results suggest that heating of the liver may efficiently induce cellular immune responses to liver cancers.

Keywords T cell · Monocyte · Cytokines · Cellular immunity · Hyperthermia · Liver cancer

Introduction

Hyperthermia (HT) has been used in combination with chemotherapy and/or radiation therapy of human malignant disorders and is considered to be a promising adjuvant therapeutic strategy for the treatment of certain types of tumors [9, 31, 33]. In parallel to the encouraging clinical observations, a large number of investigations have been performed to evaluate the ability of heat in modulating cell death, tumor blood flow, and actions of radiation therapy and antineoplastic drugs (reviewed in [12]). Furthermore, increased body temperature has been shown to stimulate the immune system through augmentation of (a) activities of T cells and NK cells, (b) production of cytokines, (c) immune responses to viral infection, and (d) mobility of leukocytes [4, 8, 12, 21, 24, 27].

The number of patients with malignant liver tumors is increasing in Japan, the vast majority of which are associated with Hepatitis C virus (HCV)/Hepatitis B virus (HBV) infection. Regional HT aimed at the liver in combination with other modalities has produced promising results in the treatment of hepatocellular carcinomas [16, 29, 35]. We have recently demonstrated that, in patients with hepatocellular carcinoma, their CD4⁺/CD8⁺ ratio of T cells and the NK-cell activity increased following the regional HT treatment [20]. Stimulation of host immune responses is considered to

Y. Kida · S. Tsuji-Kawahara (✉) · S. Kinoshita · E. Kajiwara
H. Kawabata · T. Yuasa · M. Miyazawa
Department of Immunology,
Kinki University School of Medicine, Osaka-Sayama,
Osaka, Japan
E-mail: skawa@immunol.med.kindai.ac.jp
Tel.: +81-72-3660221
Fax: +81-72-3677660

Y. Kida · S. Yukawa · M. Ichinose
Department of Internal Medicine,
Wakayama Medical University, Wakayama, Japan

V. Ostapenko · I. Nishide
Laboratory of Clinical Hyperthermia,
Shousei-kai Nishide Hospital, Kaizuka, Osaka, Japan

be a possible mechanism by which regional HT treatment, as well as systemic HT, exerts its antitumor and antiviral activities, although clear evidence is still lacking. To maximize the potential clinical benefits of the HT treatment, it is now necessary to understand thoroughly the presumed immunological effects of the regional HT. Therefore, we have focused our attention here on the effects of heating of the liver on T cells and monocytes that are involved in cellular immune responses. Our findings include a drastic decrease in blood CD14⁺ CD16⁻ inflammatory monocytes soon after the HT treatment, along with the activation of T cells. This is the first report indicating the effect of regional HT on changes in the populations of peripheral monocytes.

Materials and methods

Volunteer blood donors

Eleven healthy volunteers, five males and six females aged between 29 and 65 (average: 34.2 ± 3.4) were enrolled in the regional HT treatment or the heating of the legs and feet. All of the volunteers had no signs or symptoms of fever, infectious diseases, or immune disorders, and their leukocyte counts in peripheral blood ranged from 4,000 to 8,000 per microliter of blood. Among our subjects, one had undergone splenectomy 22 years prior to the enrollment. Some volunteers were treated with both the regional HT procedures aimed at the liver and at the lungs with an adequate interval in between. All the volunteers were given thorough explanation of the purpose, procedures, and possible risks of the experiment through written information, and have given their consent. The entire experimental procedure has been examined and approved by the Research Evaluation Committee of the Wakayama Medical College.

Hyperthermic treatment

A radio-frequency capacitive heating device Thermotron RF-8 (Yamamoto Vinita, Yao, Japan) was used to achieve regional capacitive heating of the right upper abdominal region across the liver or of the chest across the lungs as described [20]. The device has been approved as a therapeutic instrument for non-invasive HT treatment of deep-seated malignant tumors by the Ministry of Health, Labor and Welfare of Japan (Medical Device Approval No. 59B1728). Applications of this device are covered by the government's health insurance system, being regarded as a routine clinical modality [28]. Each volunteer's body was wrapped with a cooling jacket and placed between two electrodes. The effective diameter of the electrodes was 18 cm, and each enrollee received an average continuous radio-frequency irradiation of 750 W over a duration of 1 h. The estimated temperature of the liver achieved by this heating

procedure was 40°C, based on the data collected by the actual measurements of tissue temperature during HT treatment of liver tumors [16]. As an additional control group, legs and feet of four healthy volunteers were placed in a water bath and kept at 41°C for 1 h. Axillary or sublingual temperatures were measured at the end of each heating procedure in the volunteers of each group: $38.5 \pm 0.5^\circ\text{C}$ in the liver-targeted HT, $38.9 \pm 0.3^\circ\text{C}$ in the lung-targeted HT, and $37.8 \pm 0.3^\circ\text{C}$ in the leg-heating group, without significant differences in the body temperature between the groups. Vital signs including blood pressure and pulse rate were monitored during and after the HT treatment. No adverse effect due to the above heating procedures was reported, except regional irritation of the skin adjacent to the electrodes and flushing of the face, which were well tolerated.

Preparation of peripheral blood mononuclear cells (PBMC)

Blood samples were drawn from each volunteer through a subcutaneous vein in the forearm just before and soon after a 1 h HT treatment, and 1, 2, 6, 24, 36, 48, and 72 h after the end of the heating procedure. Twenty microliters of heparinized peripheral blood was collected at each time point and kept at room temperature. Within 1 h after blood collection, each peripheral blood sample was diluted with an equal volume of phosphate-buffered balanced salt solution (PBBS), and mononuclear cells were separated by density gradient centrifugation using Ficoll-Paque PLUS (Amersham Bioscience, Piscataway, New Jersey). Mononuclear cells were washed twice with PBBS, counted in a hemocytometer, and resuspended in RPMI-1640 medium supplemented with 10% fetal bovine serum (FBS) at 10^7 cells/ml.

Analyses of cell-surface markers and cell numbers

A total of 10^6 PBMC were incubated with the following combinations of fluorescent-labeled antibodies. For analyses of lymphocyte subsets, we used fluorescein isothiocyanate (FITC)-labeled anti-human CD4, FITC-labeled anti-human CD8, phycoerythrin-cyanin 5.1 (PC5)-labeled anti-human CD3, PC5-labeled anti-human CD16, FITC-labeled anti-human HLA-DR reactive to a monomorphic α -chain epitope, and PC5-labeled anti-human CD19. For staining of monocyte subsets and dendritic cells (DCs), we utilized phycoerythrin (PE)-labeled anti-human CD14, PC5-labeled anti-human CD16, FITC or PC5-labeled anti-HLA-DR, and FITC-labeled mixture of multiple lineage-specific antibodies (Lin 1; Becton-Dickinson Immunocytometry Systems, San Jose, CA, USA) that contains antibodies reactive to human CD3, CD14, CD16, CD19, CD20, and CD56 to distinguish peripheral blood DCs and basophils from other leucocytes [19, 30]. To examine the levels of T-cell activation, PE-labeled anti-human CD69 was used in combination with FITC-labeled anti-CD4 or

anti-CD8, and PC5-labeled anti-CD3. Isotype-matched mouse myeloma proteins labeled with the above fluorescent dyes were used as negative control antibodies in all analyses. All antibodies except Lin 1 cocktail were purchased from Immunotech Coulter, Marseille, France. A number of $0.3\text{--}3.5 \times 10^5$ cells stained with the antibodies were analyzed with a Becton-Dickinson FACSCalibur (Becton-Dickinson) and CellQuest software. Dead cells and debris were excluded based on their forward and side scatter profiles, and percentages of each leukocyte subpopulation among viable mononuclear cells were determined by multi-color staining with appropriate antibodies. Absolute numbers of each cell subset were then calculated by multiplying the number of total mononuclear cells with the corresponding cell percentage determined. Geometric mean fluorescence intensity for CD14 expression was obtained from the appropriate histograms for the $\text{CD14}^+ \text{CD16}^-$ subset of monocytes.

In vitro stimulation of isolated PBMC and measurements of cytokine production

A number of 8×10^5 PBMC were cultured in each well of 96-well microculture plates in RPMI-1640 medium supplemented with 10% FBS and 10 $\mu\text{g/ml}$ (final) PHA (PHA-P, Sigma Chemical Co., St. Louis, MO). After 48 h of culture at 37°C, supernates were collected, and the amounts of IFN- γ and IL-4 were measured in duplicate by an enzyme-linked immunosorbent assay using OptEIA human kits (PharMingen, San Diego, CA) according to the manufacturer's instructions.

Measurements of plasma IL-1 β and IL-6

Plasma were separated from a small aliquot of blood drawn at the same time when peripheral blood was collected for the isolation of PBMC. The concentrations of IL-1 β and IL-6 in each plasma sample were measured by using the Opt EIA human kits as described above.

Statistical analyses

The paired *t* test for samples exhibiting Gaussian distribution and the Wilcoxon's test for samples exhibiting

non-Gaussian distribution were employed to compare the values at each time-point after the HT treatment with the pre-treatment values in the same volunteer group by using the online tools archived in the Multifunctional Web Calculator established and maintained by Prof. S. Aoki, Faculty of Social and Information Studies, Gunma University, Maebashi, Japan (<http://www.aoki2.si.gunma-u.ac.jp/calculator/index.html>), and a software for statistical analysis, JSTAT, which was developed by M. Sato and downloadable from the following website: <http://www.vector.co.jp>. *P* values less than 0.05 were considered to represent statistically significant differences.

Results

Changes in the number of blood mononuclear cells following the regional HT treatment

To investigate the effects of the regional HT aimed at the liver on immune cells, we first assessed possible changes in the numbers of peripheral mononuclear cells that consist of lymphocytes, monocytes, and DCs in healthy volunteers exposed to the regional HT treatment. Following a 1 h HT treatment aimed at the liver, the absolute numbers of mononuclear cells in the peripheral blood slightly decreased throughout the 48 h of observation, although significant differences were not found in comparison with the pre-treatment value (Table 1). This change in the number of mononuclear cells was mainly due to the decrease in lymphocytes. On the other hand, there was a drastic decrease in the number of monocytes soon after the treatment in four of the six subjects who received the HT aimed at the liver. The average number of monocytes per 1 ml of blood significantly decreased from 8.5×10^4 at pre-treatment to 4.5×10^4 at 1 h post-treatment. Due to the decreased number of monocytes, a reduction in the monocyte/lymphocyte ratio was also found at 1 h post-treatment.

To evaluate whether the above changes were distinctive to the heating of the liver, the same parameters were analyzed in healthy volunteers exposed to a regional HT treatment aimed at the chest, in which the lungs were the primary target of heating, or in those received heating of the legs. No significant changes in the

Table 1 Absolute numbers and the percentages of mononuclear cells in volunteers exposed to the regional hyperthermic treatment aimed at the liver ($n = 6$)

	Cell numbers ($\times 10^4/\text{ml}$ blood)			Percent among mononuclear cells		Ratio
	Total mononuclear cells	Lymphocytes	Monocytes	Lymphocytes	Monocytes	Monocyte/lymphocyte
Pre-HT	184 \pm 31	165.1 \pm 32.1	8.5 \pm 0.8	87.2 \pm 2.3	5.4 \pm 1.1	6.4 \pm 1.4
1 h after HT	158 \pm 14	142.5 \pm 13.5	4.5 \pm 1.4*	89.2 \pm 1.3	2.8 \pm 0.8	3.2 \pm 1.0
6 h	148 \pm 15	131.5 \pm 13.9	7.6 \pm 1.7	88.6 \pm 0.5	4.8 \pm 0.6	5.4 \pm 0.7
24 h	173 \pm 29	155.2 \pm 27.3	7.9 \pm 2.0	89.4 \pm 1.2	4.6 \pm 1.0	5.2 \pm 1.2
48 h	147 \pm 9	130.4 \pm 7.7	7.2 \pm 2.1	89.0 \pm 1.6	4.7 \pm 1.2	5.4 \pm 1.3

*Significant difference ($P < 0.05$) in comparison with the pre-treatment value

number of monocytes at 1 h post-treatment were observed in any of the subjects who underwent the lung-targeted HT or the heating of the legs (data not shown), indicating a specific role of the liver in the HT-induced decrease in the monocyte numbers.

Changes in the percentages of lymphocyte subpopulations

We further investigated whether the regional HT treatment affected the percentages of lymphocyte subpopulations. In both groups of the volunteers exposed to the HT treatment aimed at the liver and that aimed at the lungs, the number of CD4⁺ T cells decreased, while that of CD8⁺ T cells was unchanged (Table 2). The CD4⁺/CD8⁺ ratio at 1 h post-treatment was reduced in five of the six subjects who received the liver-targeted HT and in all who received the lung-targeted HT treatment; however, significant differences were observed only in those whose chest was heated. Only in the volunteers exposed to the regional HT aimed at the liver, the numbers of B cells were slightly decreased at all time-points following the treatment, although the changes in comparison with the pre-treatment value were not statistically significant, and no significant changes in NK cell numbers were observed. No significant changes were observed in the subjects whose legs were heated (data not shown).

Enhancement in the activation of peripheral T cells

To examine whether T-cell functions were influenced by the regional HT treatment, we next analyzed the expression of the early activation antigen CD69 on blood T cells. Figure 1a shows representative patterns of CD69 expression in T-cell subsets before and at different time-points after the HT treatment aimed at the liver. The frequency of CD69-expressing cells in both CD4⁺ and CD8⁺ populations of T cells was significantly elevated at 1 h after the treatment in all subjects: the mean

percentages of CD69-expressing cells among CD4⁺ and CD8⁺ T cells increased by 1.7- and 1.5-fold, respectively, compared to the corresponding percentages at pre-treatment (Fig. 1b). They returned to basal levels at 6 h after the treatment, but again increased in both T-cell subsets at 24 h post-treatment, although only the changes in CD8⁺ T cells were significant. The CD69-expressing cells in both T-cell subsets showed a tendency to increase in the subjects whose lungs were heated, although there were no significant differences in comparison with the pre-treatment values. No changes in CD69 expression were found in the subjects who received the heating of the legs.

Changes in IFN- γ production from PBMC

To further evaluate the possible effect of the regional HT treatment on T-cell activation, cytokine productions from PBMC were also analyzed. PBMC collected before and at different time-points after the treatment were stimulated with PHA, and the accumulation of interferon (IFN)- γ and interleukin (IL)-4 in the medium during 48 h of cell culturing was measured. In the volunteers who received the liver-targeted HT, the amount of IFN- γ produced gradually and significantly increased in the 2 days following the heating procedure, peaking at 36 h after the end of the HT treatment (Fig. 2a). In the subjects exposed to heating of the lungs or the legs, there were no significant changes in the PHA-induced production of IFN- γ . On the other hand, the amount of IL-4 produced after PHA stimulation showed no change at all during the 3 days of observation in all groups (Fig. 2b).

Elevation of plasma cytokine levels

Plasma levels of proinflammatory cytokines, IL-1 β and IL-6 were measured before and following the regional HT. In subjects who underwent HT aimed at the liver, both cytokines showed no significant change immedi-

Table 2 Absolute numbers ($\times 10^4$ /ml blood) of lymphocyte subsets in volunteers exposed to the regional hyperthermic treatment

	CD4 ⁺ T	CD8 ⁺ T	CD4 ⁺ /CD8 ⁺	B (CD19 ⁺)	NK (CD16 ⁺ HLA-DR ⁻)
Liver-targeted HT (<i>n</i> = 6)					
Pre-HT	71.8 \pm 20.0	28.3 \pm 3.8	2.4 \pm 0.4	20.6 \pm 6.8	16.5 \pm 4.0
1 h after HT	55.6 \pm 6.8	28.8 \pm 4.9	2.1 \pm 0.4	14.9 \pm 2.2	17.2 \pm 3.0
6 h	52.0 \pm 6.8	24.3 \pm 3.0	2.2 \pm 0.3	15.1 \pm 2.6	16.8 \pm 4.4
24 h	65.9 \pm 17.3	28.5 \pm 4.2	2.3 \pm 0.4	15.6 \pm 2.5	17.8 \pm 3.7
48 h	49.7 \pm 5.0	24.4 \pm 3.9	2.4 \pm 0.5	16.4 \pm 2.0	16.9 \pm 3.2
Lung-targeted HT (<i>n</i> = 5)					
Pre-HT	63.5 \pm 9.8	27.8 \pm 5.3	2.6 \pm 0.6	15.4 \pm 3.2	16.1 \pm 1.2
1 h after HT	54.6 \pm 8.8	29.9 \pm 7.4	2.1 \pm 0.4*	15.9 \pm 3.7	15.5 \pm 2.3
6 h	60.2 \pm 12.2	24.9 \pm 6.1	2.7 \pm 0.6	14.7 \pm 4.9	11.6 \pm 2.4
24 h	58.0 \pm 11.4	26.2 \pm 4.6	2.4 \pm 0.5	18.6 \pm 5.6	16.4 \pm 1.7
48 h	50.4 \pm 7.9	24.4 \pm 3.8	2.2 \pm 0.4	09.1 \pm 2.8	13.8 \pm 2.9

*Significant difference (*P* < 0.05) in comparison with the pre-treatment value

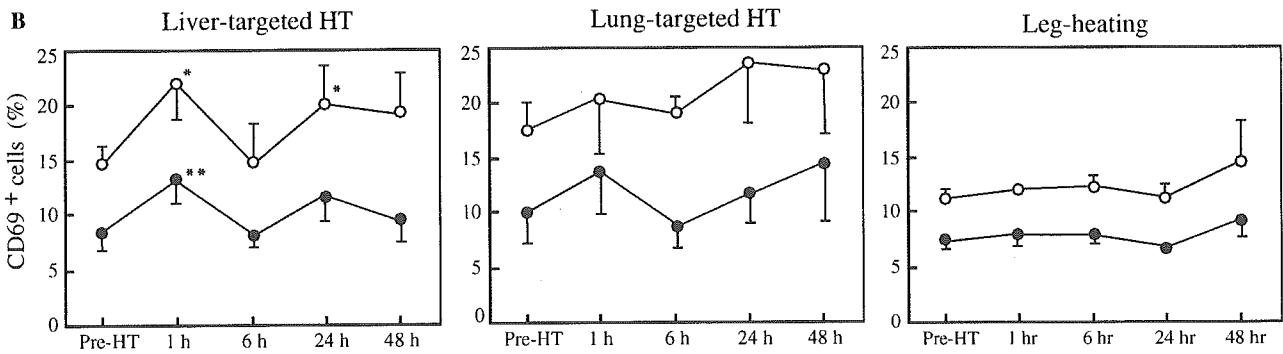
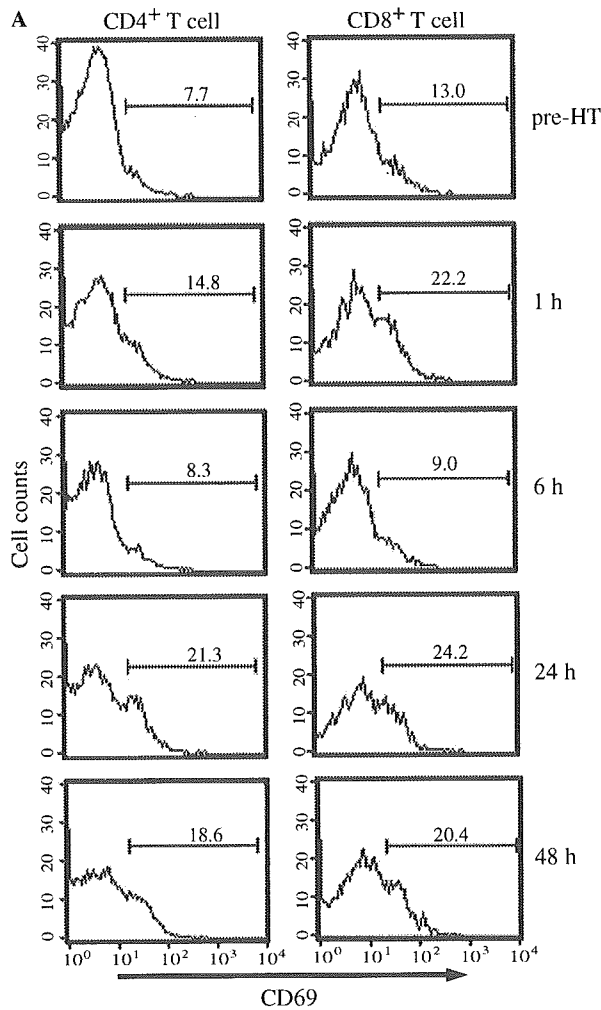


Fig. 1 Effects of regional hyperthermic treatment aimed at the liver on peripheral T-cell activation. PBMC were prepared before and at the indicated time-points after the 1 h HT treatment aimed either at the liver or at the lungs, or after 1 h heating of the legs, and CD69 expression on CD4⁺ and CD8⁺ T cells was monitored by flow cytometry. **a** Histograms showing CD69 expression on each T-cell subset in a representative volunteer who received the liver-targeted HT treatment. Numbers indicate the percentage of CD69-positive

cells. **b** Time course of CD69 induction on CD4⁺ (closed circles), and CD8⁺ (open circles) T cells after the HT treatment aimed at the liver (left panel) or at the lungs (middle panel), or heating of the legs (right panel). Each circle and bar show a mean \pm SEM calculated from the data obtained from four to six volunteers. *Significantly different from the mean value observed before the HT treatment, $P < 0.05$; **significantly different from the same pre-treatment value, $P < 0.01$

ately after the treatment, but continued to increase gradually towards the end of the observation period, exhibiting significant differences at 24 and 48 h post-

treatment (Fig. 3). Again, no changes in the plasma cytokine levels were found in the volunteers who underwent heating of the lungs or the legs.

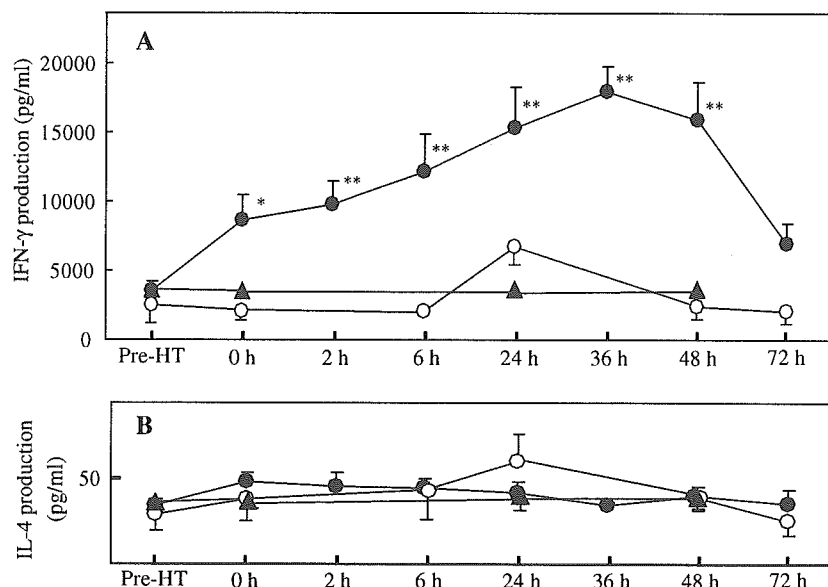


Fig. 2 Changes in PHA-induced cytokine production from cultured PBMC after the 1 h regional HT aimed either at the liver (closed circles) or at the lungs (open circles), or after 1 h heating of the legs (closed triangles). PBMC prepared from each subject at each indicated time-point were stimulated with PHA, and the concentrations of IFN- γ (a) and IL-4 (b) produced into culture

medium were measured after 2 days of incubation. Each symbol and bar show mean \pm SEM calculated from the data obtained from 4 to 11 volunteers. * Significantly different from the mean value observed before the HT treatment, $P < 0.02$; **significantly different from the same pre-treatment value, $P < 0.01$

Changes in the numbers of monocyte subsets

Recently, functional heterogeneity of human blood monocytes has been demonstrated based on the expression levels of the lipopolysaccharide (LPS) receptor CD14 and the Fc γ receptor III (CD16) [10]: CD14⁺CD16⁻ cells that correspond to classical inflammatory monocytes and CD14^{lo}CD16⁺ cells that have been characterized as resident monocytes (Fig. 4a). As shown in Table 1, a marked reduction in the number of the whole monocyte population in the peripheral blood was observed following the HT treatment aimed at the liver. In order to examine which subset among the monocytes was affected by the treatment, we further analyzed both frequencies and absolute numbers of the above monocyte subsets as well as those of DCs which also exist within the blood monocyte population defined by conventional gating based on the forward and side scatter profiles (Fig. 4b). The DC population was distinguished in the present study by their expression of HLA-DR and the lack of the expression of CD3, CD14, CD16, CD19, CD20, and CD56. At 1 h after the liver-targeted HT, the frequency of CD14⁺CD16⁻ cells among the gated monocyte population was markedly reduced in five of the six volunteers, the mean values of which were $87.0 \pm 1.4\%$ at pre-treatment and significantly lower $76.2 \pm 4.2\%$ at 1 h after the HT treatment. A remarkable reduction in the absolute number of CD14⁺CD16⁻ monocytes was also observed at 1 h post-treatment. In contrast to the sharp decrease in the percentage of CD14⁺CD16⁻ monocytes, CD14^{lo}CD16⁺ monocytes increased significantly in their percentage at 1 h after the

liver-targeted HT treatment. However, due to the decrease in the total number of peripheral monocytes (Table 1), their absolute numbers were unchanged. With respect to DCs, their number tended to decrease soon after the HT treatment, and remained low throughout the 48 h of observation following the heating of the liver. There were no significant changes in the frequencies and absolute numbers of monocyte subsets in volunteers exposed to the lung-targeted HT. In addition, cell surface expression of CD14 molecules on the CD14⁺CD16⁻ monocytes increased starting from 6 h following the heating procedure, exhibiting significant differences ($P < 0.05$) at 6 and 24 h post-treatment in the liver-targeted HT, and at 6 h post-treatment in the lung-targeted HT group (Fig. 4c). No significant changes in the monocyte-counts or the CD14 expression were observed in the volunteers exposed to the heating of the legs (data not shown).

Discussion

The findings described herein provide evidence that the regional HT treatment aimed at the liver induces activation of peripheral T cells, production of proinflammatory cytokines, and changes in the number of blood monocyte subpopulations and their CD14 expression. To heat the liver selectively in the present study, we placed a pair of electrodes on the front and back of the subject's right upper abdominal region; however, it is also conceivable that other lymphoid organs that lie adjacent to the liver might have been heated. With

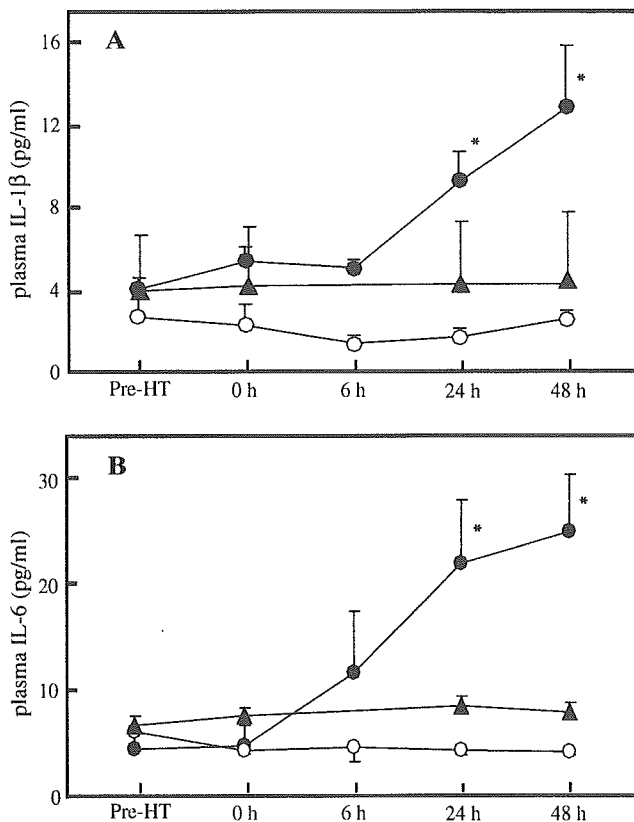


Fig. 3 Average plasma concentrations of IL-1 β (a) and IL-6 (b) after the 1 h regional HT aimed either at the liver (closed circles) or the lungs (open circles), or after 1 h heating of the legs (closed triangles). Each symbol and bar represent mean \pm SEM calculated from the data obtained from 4 to 11 volunteers. *Significantly different from the mean value observed before the HT treatment, $P < 0.01$

respect to the spleen, however, there happened to be a volunteer who had undergone splenectomy among our subjects. Importantly, we observed the same changes in the above immunological parameters in the splenectomized volunteer following the HT aimed at the liver, ruling out the possibility that the effects of the right upper abdominal heating depend on the presence of the spleen. When administering HT to the chest, in which the lungs were supposed to be the primary target organs, the subject's body temperatures reached levels as high as those measured in the volunteers treated with the liver-targeted HT; however, the lung-targeted treatment resulted in no significant activation of T cells (Figs. 1 and 2) or changes in the numbers of blood monocyte subsets (Fig. 4). Thus, it is highly conceivable that the changes observed following the heating of the right upper abdominal region can be mainly attributed to the heating of the liver.

Immunological changes in humans who received systemic hyperthermic treatment have been described, most of which refer to its effect on the composition of lymphocyte subpopulations, the concentration of serum cytokines, and the NK cell activity (reviewed in [12]). On

the other hand, there are very few reports describing the effect of regional HT on the host's immune system. Regarding the changes in lymphocyte subpopulations, we observed a slight decrease in the peripheral CD4⁺/CD8⁺ ratio following the HT treatment aimed at the liver and lungs, which was statistically significant in the latter case. The decrease in CD4⁺/CD8⁺ ratio is mainly accounted for by the reduction in the number of CD4⁺ T cells, rather than an increase in CD8⁺ T-cell counts, in the both experimental groups. In line with this result, a decrease in CD4⁺/CD8⁺ ratio has been shown in patients with hepatocellular carcinoma immediately after the regional HT at the upper abdominal region [20], as well as in the persons who underwent whole-body hyperthermia (WBH) [1, 7]. By way of experiment with mice, WBH has been shown to enhance the homing of antigen-specific T cells to the inflammatory site; however, differences in sensitivity to this treatment of each T-cell subset have not been described [21]. As a possibility, chemotaxis of CD4⁺ T cells into tissues might be more quickly and markedly affected by heat than that of CD8⁺ T cells, thus resulting in the sharp decrease in CD4⁺/CD8⁺ ratio we observed.

In the present study, T-cell activation was assessed by the expression of the activation marker CD69 and by the generation of cytokines after the stimulation with PHA. CD69 molecule is a phosphorylated and disulfide-linked 27/33 kD homodimeric protein [26], and signals triggered by anti-CD69 antibodies result in the synthesis of different cytokines and their receptors, and the enhancement of T cell proliferation [5, 17]. The expression of CD69 on human T cells is induced in vitro by a wide variety of stimuli: an increase in CD69 expression is observed at as early as 1–4 h after stimulation with anti-CD3 antibody or polyclonal mitogens including phorbol ester 12-myristate 13-acetate (PMA), an activator of intracellular protein kinase C (PKC), whereas it takes 24–72 h after an in vitro stimulation through antigen-T-cell receptor interactions for the induction of CD69 expression [5, 11]. In the volunteers exposed to the HT treatment aimed at the liver, we observed the increase in the fraction of CD69-expressing cells in both CD4⁺ and CD8⁺ populations of T cells in two waves (Fig. 1). The first elevation, accompanied by the nearly twofold increase in PHA-induced IFN- γ production (Fig. 2a), was found at 1 h after the liver-targeted HT treatment. Based on the above knowledge, this "early phase" of T-cell activation, as demonstrated by the CD69 expression, is not attributable to an antigen-dependent reaction. Our observation is rather consistent with a report demonstrating that the expression of CD69 molecule on the surface of resting human T cells was induced at as early as 1 h after an incubation at 44°C for 30 min, which subsided 3 h later, due to a rapid translocation of the molecules already present in the cell cytoplasm [23]. In addition, fever-range (39.5°C) WBH has been shown to result in a rapid increase in PKC activity within T cells [32]. Thus, the liver-targeted HT treatment may have caused the very early induction of CD69 molecules to

the cell surface via yet undescribed PKC signal transduction pathways, which in turn lead to the observed T-cell activation and the resultant increase in IFN- γ production. Of note, an extreme WBH of 41.8–42.2°C has led to a reversible and transient immune impairment in the patients with metastatic cancers during or immediately after the heating procedure [1, 4]. The regional heating aimed at the liver may have an advantage in that no intense immune impairment is induced during the treatment.

On the other hand, the “late phase” of CD69 induction was observed at 24 h post-HT treatment aimed at the liver. At the same time-point, a more than threefold increase in IFN- γ production from the PHA-stimulated PBMC was observed as compared to the pre-treatment value, suggesting that the peripheral T cells were fully activated at 24 h after the HT treatment of the liver. Furthermore, the plasma concentrations of IL-1 and IL-6, which are known to be secreted predominantly from vascular endothelial cells and professional phagocytes and act on the activation of lymphocytes [2, 6], were also elevated in our volunteers at this time-point, while there were no significant elevations in the early phase. In contrast, the plasma IL-6 increased during or just after the heating treatment in patients treated with an extreme WBH of 41.8°C, and returned to basal levels at 24-h post-treatment [4, 25]. The rapid increase in plasma IL-6 may be attributable to an augmentation in IL-6 release from the circulating monocytes or T cells. In fact, the TNF- α release from PBMC has been shown to increase immediately after the WBH [36]. On the other hand, the increase in plasma IL-6 was observed only in the subject who received the liver-targeted HT, but not in those receiving the heating of the lungs or legs, at the late phase. Liver cells can secrete a variety of cytokines including IL-1, IL-6 and TNF- α [2]. Among these, TNF- α is a potent inducer of IL-1 and IL-6 expression [2, 14]. Interestingly, the HT treatment has been shown to enhance TNF- α release from Kupffer cells in LPS-challenged mice [13]. It is possible, therefore, that the TNF- α locally produced by the HT-treated hepatic tissue may have, in turn, stimulated IL-1 and IL-6 release from the liver cells, which resulted in the observed late-phase increases in the plasma cytokines.

Unprecedented heterogeneity in their surface marker phenotypes and functions of blood monocytes has been demonstrated only recently: classical CD14⁺ CD16⁻ monocytes that migrate into the sites of inflammation, where they differentiate into macrophages and DCs, and CD14^{lo} CD16⁺ monocytes that extravasate into tissues, where they serve as specific resident myeloid cells such as Kupffer cells, alveolar macrophages, or Langerhans cells [10, 37]. Interestingly, our study revealed a remarkable decrease in only the CD14⁺ CD16⁻ monocyte subset in the peripheral blood, but not in the CD14^{lo} CD16⁺ monocytes and circulating DCs, at 1 h after the HT treatment. So far, there have been no reports demonstrating the decrease in the number of monocytes by HT treatment, whereas an increased number of total

monocytes has been shown in the peripheral blood of healthy volunteers at 6 h after a fever-range WBH treatment [36]. Our observation raises two possibilities for the action of the heating of the liver: (1) apoptotic loss of the peripheral CD14⁺ CD16⁻ monocytes may have been selectively induced, or (2) the entrance of CD14⁺ CD16⁻ monocytes into tissues such as the liver may have been facilitated, resulting in their disappearance from the peripheral blood. Regarding the heat-induced apoptosis, a number of experiments both in vitro and in vivo have shown that HT treatments influence cell viability in various types of tumors [3, 34]. Exposing monocytes to 41°C for 1 h, however, had only a minor effect on their viability [22]. We also observed no effect of an in vitro treatment at 40°C for 1 h on the viability of blood monocytes (S. Kinoshita et al. unpublished observation). Taken together, it is not likely that the decrease in blood monocytes at 1 h post-HT treatment is due to a heat-induced apoptosis. With respect to the other hypothesis concerning the trafficking of CD14⁺ CD16⁻ monocytes, chemokines produced locally in the liver should be taken into consideration. It has recently been reported in fulminant hepatic failure that the expression of intrahepatic chemokines, MCP-1, MIP-1 α , MIP-1 β , and RANTES, which are produced from Kupffer cells, sinusoidal endothelial cells, and hepatocytes, was closely correlated with the extent of infiltration by macrophages or monocytes and T cells into the liver [15]. Moreover, mRNAs of these intrahepatic chemokines have started to be expressed as early as 1 h after an administration of toxins which elicit liver damage in mouse models of fulminant hepatic failure [15]. Of note, inflammatory chemokine receptors, CCR1, CCR2, and CCR5, which bind to MCP-1, MIP-1 α , MIP-1 β , and RANTES, are expressed on human CD14⁺ CD16⁻ monocytes at much higher levels than on CD14^{lo} CD16⁺ monocytes [10]. Collectively, the heat-exposed liver may produce the above-described inflammatory chemokines immediately after an HT treatment, resulting in the entrance into the liver of blood CD14⁺ CD16⁻ monocytes. Further, upregulation of the CD14 expression levels on the CD14⁺ CD16⁻ monocytes in the blood was found at as early as 6 h following the liver-targeted HT treatment, and this increase lasted at least until 24 h post-HT (Fig. 4). In contrast to the above result, a short-lasting increase in the CD14 expression on monocytes was observed in healthy volunteers exposed to fever-range WBH [36] and in our volunteers treated with the lung-targeted HT. The CD14 expression level on the monocytes was associated with an ability to release TNF- α following the stimulation with LPS [36]. Taken together, the possible early migration of CD14⁺ CD16⁻ monocytes into the heated liver may have contributed to the observed long-lasting activation of peripheral monocytes after the HT treatment and the observed increase in plasma levels of IL-1 β and IL-6.

As there is still not enough evidence demonstrating substantial direct anticancer effect of regional HT when